



Accumulation of endogenous adenosine improves cardiomyocyte metabolism via epigenetic reprogramming in an ischemia-reperfusion model

Peng Wang^{a,b,1}, Rifeng Gao^{a,d,1}, Tingting Wu^{c,1}, Jinyan Zhang^a, Xiaolei Sun^{a,b}, Fan Fan^{a,b}, Cong Wang^{a,b}, Sanli Qian^{a,b}, Bingyu Li^{a,b}, Yunzeng Zou^{a,b}, Yuqing Huo^g, John Fassett^e, Yingjie Chen^f, Junbo Ge^{a,b}, Aijun Sun^{a,b,*}

^a Shanghai Institute of Cardiovascular Diseases, Zhongshan Hospital, Fudan University, Shanghai, China

^b Department of Cardiology, Zhongshan Hospital, Fudan University, Shanghai, China

^c Department of Neurology, Zhongshan Hospital, Fudan University, Shanghai, China

^d Cardiac Surgery Department, The Second Affiliated Hospital Zhejiang University School of Medicine, China

^e Department of Pharmacology and Toxicology, University of Graz, 8010, Graz, Austria

^f Department of Physiology & Biophysics, University Mississippi Medical Center, MS, 39216, USA

^g Vascular Biology Center, Department of Cellular Biology and Anatomy, Medical College of Georgia, Augusta University, Augusta, GA, USA

ARTICLE INFO

Keywords:

Adenosine
Ischemia-reperfusion
ADK
IGF-1
Epigenetics
Metabolism

ABSTRACT

Adenosine kinase (ADK) plays the major role in cardiac adenosine metabolism, so that inhibition of ADK increases myocardial adenosine levels. While the cardioprotective actions of extracellular adenosine against ischemia/reperfusion (I/R) are well-established, the role of cellular adenosine in protection against I/R remains unknown. Here we investigated the role of cellular adenosine in epigenetic regulation on cardiomyocyte gene expression, glucose metabolism and tolerance to I/R. Evans blue/TTC staining and echocardiography were used to assess the extent of I/R injury in mice. Glucose metabolism was evaluated by positron emission tomography and computed tomography (PET/CT). Methylated DNA immunoprecipitation (MeDIP) and bisulfite sequencing PCR (BSP) were used to evaluate DNA methylation. Lentiviral/adenovirus transduction was used to overexpress DNMT1, and the OSI-906 was administered to inhibit IGF-1. Cardiomyocyte-specific ADK/IGF-1-knockout mice were used for mechanistic experiments. Cardiomyocyte-specific ADK knockout enhanced glucose metabolism and ameliorated myocardial I/R injury *in vivo*. Mechanistically, ADK deletion caused cellular adenosine accumulation, decreased DNA methyltransferase 1 (DNMT1) expression and caused hypomethylation of multiple metabolic genes, including insulin growth factor 1 (IGF-1). DNMT1 overexpression abrogated these beneficial effects by enhancing apoptosis and decreasing IGF-1 expression. Inhibition of IGF-1 signaling with OSI-906 or genetic knocking down of IGF-1 also abrogated the cardioprotective effects of ADK knockout, revealing the therapeutic potential of increasing IGF-1 expression in attenuating myocardial I/R injury. In conclusion, the present study demonstrated that cardiomyocyte ADK deletion ameliorates myocardial I/R injury via epigenetic upregulation of IGF-1 expression via the cardiomyocyte adenosine/DNMT1/IGF-1 axis.

1. Introduction

Acute myocardial ischemia, resulting from arterial thrombosis, severely depresses cardiac contractile function. Paradoxically, while thrombolysis and reperfusion of the ischemic tissue is necessary to restore cardiomyocyte contractile function, a significant portion of the

cell injury and death occur in response to reperfusion. The cardiac injury imposed by ischemia and reperfusion is defined as cardiac ischemia-reperfusion (I/R) injury, and contributes to the long-term poor prognosis in ischemic heart disease [1]. Ischemic heart disease resulting from I/R injury is associated with high morbidity [2]. Therefore, identifying cell and molecular mechanisms that contribute to cardiomyocyte death

* Corresponding author. Room 205, Building No.19, No. 18 of Road Fenglin, District Xuhui, Shanghai, USA.

E-mail address: wang.peng1@zs-hospital.sh.cn (P. Wang).

¹ These authors contributed equally to this work.

after reperfusion will be critical for development of adjunctive therapies for myocardial infarction.

Adenosine is a purine nucleoside produced during cellular stress conditions such as inflammation, diabetes, and methionine cycle [3–5]. Adenosine activation of adenosine receptors or related kinase regulation exert important protective effects, including protection against ischemia/reperfusion injury [6,7], reduction of oxidative stress [8], improved coronary flow/cardiac perfusion [9], regulation of inflammatory response [10,11], and attenuation of hypertrophy and heart failure during pressure overload [12]. Despite extensive evidence, however, that adenosine receptor activation can attenuate I/R injury in cell and animal models, the protective effects of adenosine receptor agonists, as well as other preconditioning or post-conditioning agents, have failed to translate into clinical practice [13]. Thus, there is a clinical unmet need for identification of novel targets for attenuating reperfusion injury.

Adenosine kinase (ADK) plays a major role in cardiomyocyte adenosine metabolism, so that its inhibition results in cellular adenosine accumulation and release of adenosine into the interstitial space [14, 15]. While the cardioprotective roles of extracellular adenosine are established, the impact of cellular adenosine in cardioprotection is not clear. As a byproduct of s-adenosyl homocysteine (SAH) hydrolysis, adenosine can inhibit s-adenosylhomocysteine hydrolase (SAHH) activity, causing SAH to accumulate [16]. Because SAH is a potent inhibitor of methyltransferase activity, inhibition of SAHH by cellular adenosine results in increased SAH to s-adenosylmethionine (SAM) ratio and can diminish DNA methylation [17,18]. While epigenetic effects of ADK disruption have been observed in several cells and tissues, the role of ADK and cellular adenosine in cardiomyocyte DNA methylation and cardioprotection are unknown.

Recently, cross-talk between metabolism and epigenetics has been identified as a potential target for the treatment of cardiovascular diseases [19,20], and several studies have indicated a dynamic relationship between metabolic processes and gene expression [21,22]. Furthermore, cellular metabolites, such as methyl and flavin adenine dinucleotide (FAD), have been shown to induce permanent alterations in cellular morphology and genetic structure in multiple disease models [23,24], likely dependent upon epigenetic modifications. This phenomenon is referred to as metaboloepigenetics.

In this study, we investigated the role of ADK in cardiomyocyte DNA methylation, gene expression and cardioprotection against I/R in cardiomyocytes. Our findings indicate that inhibition of ADK protected heart against I/R injury by modulating epigenetic-metabolic crosstalk in cardiomyocytes.

2. Methods

The data, analytical methods, and study materials that support the findings of this study are available from the corresponding author upon reasonable request.

2.1. Bioinformatic analysis to identify potential metabolic genes

Raw data or series matrix files for microarray datasets were downloaded from the public Gene Expression Omnibus (GEO) database. The microarray sequencing results were derived from I/R samples of each group to reduce heterogeneity within the analysis. Analysis was performed for the corresponding annotation documents, pathway/process enrichment, and protein interactions identified by Search Tool for the Retrieval of Interacting Genes/Proteins (STRING) to transform the probes into gene symbols, while BioGPS tools were used to detect ADK expression in different tissues or organs as previously described [22].

2.2. Transgenic mice and animal experiments

Cardiomyocyte-specific ADK-knockout mice (ADK-Cre) were generated as previously described [12] (Fig. S12), and cardiomyocyte-specific

insulin-like growth factor 1 (IGF-1)-knockout mice were purchased from Shanghai Model Organisms Center, Inc. These two mouse strains were crossed to establish cardiomyocyte-specific ADK/IGF-1 double-knockout mice. Myocardial I/R surgery was performed in the mice as previously described [25]. Briefly, mice were anesthetized by a facemask connected to ventilator (2% isoflurane mixed with 100% O₂, volume: 2 L/min, frequency: 60/minute). For each mouse, a left thoracic incision was made to expose the heart. Myocardial ischemia was induced by tying a slipknot around the left anterior descending coronary artery with a 6.0 silk suture (Surgical Specialties Corporation, England). After 30 min, the slipknot was released to allow reperfusion. Reperfusion times varied based on the experiment being performed. Reperfusion times ranged between 3 h and 24 h for investigation of adenosine-associated methylation levels. IGF-1R inhibitor (OSI-906, 10 mg/kg) was administered to mice via intragastric delivery, and DNMT1 adenovirus was administered via tail vein injection. To explore detailed changes *in vivo*, the specific cell sub-population were harvested and prepared immediately for further experiments, the details of protocols were described in supplementary files.

2.3. Echocardiography

Mice were anesthetized with 1% pentobarbital after myocardial I/R surgery, and two-dimensional transthoracic echocardiography was conducted in a standard setting using a 30-MHz high-frequency scan head (VisualSonics Vevo770; VisualSonics Inc., Toronto, ON, Canada) as previously described [22]. The left ventricular internal dimension at diastole (LVIDd), left ventricular internal dimension at systole (LVIDs), left ventricular end-diastolic volume (LVEDV), and left ventricular end-systolic volume (LVESV) were measured for each mouse, and the left ventricular fractional shortening (FS) and ejection fraction (EF) were calculated using Simpson's rule (Fig. S13E). All parameters were measured by an experienced echocardiographer who was blinded to the treatment protocol (Supplementary Table 4).

2.4. Evans blue and 2,3,5-triphenyltetrazolium chloride (TTC) staining

Mice were sacrificed at 3- and 24-h after I/R surgery, and the hearts were quickly sectioned for Evans blue and TTC staining as previously described [22]. Evans blue staining was used to assess the risk zones, and TTC staining was used to measure the areas of the infarcted tissue and entire left ventricle. Analysis was conducted using ImageJ software as previously described [22].

Assessment of ADK expressions, adenosine levels, SAM/SAH-associated metabolites, global DNA methylation, DNMT1 activity and specific histone methylation.

Quantitative measurements of cellular adenosine, SAM/SAH-associated metabolites were assessed by reversed-phase HPLC on freshly isolated cells obtained through the sub-population isolation method, and isolated cardiomyocytes were cultured and verified by commercial kits. Relative amounts were calculated with the average OD of wild type as respective reference in our study for ELISA experiment. The ADK expressions, ADK activity, global DNA methylation, DNMT1 activity and specific histone methylation were determined using commercial kits according to the manufacturer's instructions. The detailed information of kits was presented in Supplementary Table 1. The HPLC assay method is detailed in the Appendix Supplementary Method.

2.5. Detection of adenine nucleotide related metabolites

The cAMP concentrations were determined using a Cyclic AMP XP® assay kit (Cell Signaling Technology, Danvers, MA, USA) according to the manufacturer's protocol. AMP, ADP, ATP and adenine were measured by liquid chromatography (LC)-mass spectrometry (MS) analysis, and the details were provided in Appendix Supplementary Method.

2.6. Terminal transferase-mediated dUTP nick end-labeling (TUNEL) assay

Myocardial tissue sections after I/R surgery were stained using a fluorescein-conjugated TUNEL *in situ* cell death detection kit (Roche, Catalog No. 11684795910). Procedures were performed according to manufacturer's instructions. The number of TUNEL-positive cells was determined in 10 independent fields for each sample.

2.7. Hypoxia/reoxygenation (H/R) injury cell model

The H/R injury cell model was established as previously described [25]. Briefly, healthy adult mouse ventricular cardiomyocytes were isolated (Details in supplementary appendix files), or HCM-a human cardiomyocyte were cultured for ADK overexpression experiment. Cells for *in vivo* experiments were further under isolation and prepared for test immediately, while cells for *in vitro* experiments cultured in laminin-coated dishes in a standard tissue culture incubator (37 °C, 5% CO₂) for 24 h. Then, the cardiomyocytes were placed in hypoxic buffer (118 mmol/L NaCl, 24 mmol/L NaHCO₃, 1 mmol/L NaH₂PO₄, 2.5 mmol/L CaCl₂·2H₂O, 1.2 mmol/L MgCl₂, 20 mmol/L sodium lactate, 16 mmol/L KCl, and 10 mmol/L 2-deoxyglucose [pH 6.2]) and placed in a hypoxia incubator (1% O₂, 94% N₂, 5% CO₂). Reoxygenation was achieved by replacing the hypoxic buffer with fresh culture medium and incubating the cells in a standard tissue culture incubator for the indicated time [25]. The cells and their supernatants were harvested separately after reoxygenation. Further adenosine supplementation is 10 μmol/L, and lentivirus transduction was performed for DNMT overexpression *in vitro*.

2.8. Flow cytometry

Isolated cardiomyocytes (10⁷ cells) were trypsinized for 5 min and then resuspended and stained using an apoptosis detection kit (BD, Catalog No. 559763). The samples were incubated for 60 min at 4 °C in the dark, and washed three times with a flow cytometry staining buffer. Apoptotic cells were detected using a BD LSRFortessa Cell Analyzer, and data were analyzed with FlowJo software.

2.9. Western blot

Protein lysates were prepared from isolated cardiomyocytes or from the infarction border zone tissues isolated from mice after I/R surgery according to previously established protocols. Samples containing an equal amount of protein were separated by SDS-polyacrylamide gel electrophoresis (SDS-PAGE) and transferred to nitrocellulose membranes (Millipore). The membranes were blocked with 5% bovine serum albumin (BSA) in Tris-buffered saline for 1 h prior to overnight incubation with the respective primary antibodies at 4 °C. Levels of target proteins were analyzed with β-actin (1:5000) as the loading control. The detailed information of antibodies are described in [Supplementary Table 2](#).

2.10. Real-time quantitative polymerase chain reaction (qPCR)

Total RNA was isolated from myocardial tissues or cardiomyocytes, and any contaminating genomic DNA was removed by DNase digestion. Complementary DNA (cDNA) was synthesized from 1 μg total RNA at 37 °C for 60 min in a 20-μL reaction system (Superscript III). The data were analyzed for the target genes. The primers used for qPCR are provided in the [Supplemental Table 3](#).

2.11. Methylated DNA immunoprecipitation (MeDIP)-qRT-PCR and bisulfite PCR for IGF-1 promoter

MeDIP-qRT-PCR was carried out with a Magnetic Methylated DNA

Immunoprecipitation kit (Diagenode, Denville, NJ, USA). The MeDIP DNA was used for qPCR. Bisulfite PCR was performed to detect IGF-1 promoter methylation. Details were performed as described in the Appendix Supplementary Method. The primers used for BSP are provided in the [Supplemental Table 3](#).

2.12. Lentivirus/adenovirus production and transduction

The full-length sequences of the DNMT1 gene were produced by PCR. The set of primers were as follows (forward primer: GCGAATTC-GAAGTATACCTCGAGGCCACCATGGCTGCCAAACGGAGACC; reverse primer: CATGGTCTTTGTAGTCCATGGATCCGTCCTTGGTAGCAGCCTCCTCTTT). The products of the DNMT1 gene were amplified, purified, digested and ligated into the respective sites in the PGMLV-6395 vector (Genomeditech, China). 10 μg DNMT1 over-expression vectors were mixed with 10 μl Lenti-HG mix and 60 μl HG transgene reagent (Genomeditech, China) for the lentivirus package, and transfection of 293 T cells was performed with Lipofectamine 2000 reagent (Invitrogen, Thermo Fisher Scientific, USA). 100X Enhancing buffer (Genomeditech, China) was used for better transfection efficiency after 12 h incubation. The virus-containing supernatants were collected after 48 h transfection, and then transformed with 0.22 μm cellulose acetate filters (Merck Millipore, USA) for ultracentrifugation. For transductions, the respective Lentivirus (1 × 10⁶ PFU/mL in culture medium) was incubated with cardiomyocytes (10⁵ cells/mL) for 48 h, and the transduction efficiency was analyzed by Western blot.

As for adenovirus, the same over-expression sequences were used as the Lentivirus production, and adenovirus was established with routine protocols. In short, the products of the DNMT1 gene were cloned into the vector. The vectors were then packaged into a recombinant adenovirus using U293 cells (Invitrogen, Carlsbad, USA) according to the manufacturer's instructions. In control group, the mice were injected with ADV-NC (1 × 10¹⁰ infectious units/mouse) by tail vein. In DNMT1 overexpression group, the mice were infected with ADV-DNMT1(1 × 10⁹ infectious units/mouse) by tail vein.

2.13. Immunostaining and immunofluorescence analyses

For histological analyses, myocardial tissues were serially cryosectioned at a 5-μm thickness and mounted onto slides. The cryosections were fixed in 4% paraformaldehyde for 30 min and then rinsed in PBS. Plasma membranes were permeabilized with Triton X-100 (Sigma, St. Louis, USA). Nonspecific binding sites were blocked by incubation with 5% BSA (Sigma, St. Louis, USA) in PBS for 1 h. The slides were then incubated with primary antibodies overnight at 4 °C. Then, the slides were rinsed and incubated with secondary antibodies at room temperature for 2 h. The stained slides were photographed with an Olympus IX71 or Zeiss Pascal confocal microscope.

2.14. Detection of glucose metabolism

Quantitative measurements of glucose metabolism were performed with commercial kits according to the manufacturer's instructions. The kit information is described in [Supplementary Table 1](#).

Preparation of fluorine-18 (18 F)-labeled positron emission tomography (PET) probes and micro-PET/computed tomography (CT) imaging.

Standard 18 F-labeled fluorodeoxyglucose (FDG) and 4 (R, S)-[18 F] fluoro-6-thia-heptadecanoic acid (FTHA) probes were prepared on the same day of examination by the Department of Nuclear Medicine, Fudan University Shanghai Cancer Center. Each probe was prepared according to a standard protocol, and quality control analysis was conducted to ensure that they met the radiopharmaceutical requirements as previously reported [26]. Micro-PET/CT scanning and image analysis were performed with an Inveon micro-PET/CT system (Inveon Research Workplace, Siemens Medical Solution, California, USA). Each mouse

was intraperitoneally injected with approximately 200 μ Ci of the 18 F-labeled probe. Then, 1 h after injection, a 20-min static scan was acquired for each mouse while under isoflurane anesthesia. Mice were fasted overnight prior to injection and were kept under isoflurane anesthesia during the 1-h period prior to imaging. Images were reconstructed and standardized uptake values were quantified from regions of interest (ROIs) using Inveon Research Workplace after recalibration according to the percentage of the injected dose per gram of tissue (ID/g %).

2.15. S-adenosylhomocysteine hydrolase (SAHH) activity assay

SAHH activity was assessed using the adenosylhomocysteinase activity fluorometric assay kit (Abcam, ab197002, USA) per the manufacturer’s instructions. SAHH catalyze hydrolysis of SAH to homocysteine and adenosine.

2.16. Statistical analysis

Data were presented as the mean \pm standard error of the mean (SEM). Significance between comparisons was determined by one-way analysis of variance (ANOVA) followed by Tukey’s post-hoc test or a two-tailed Student’s t-test. A p-value<0.05 was considered statistically significant.

3. Results

3.1. I/R resulted in the upregulation of ADK in the acute period

RNA sequencing was performed to detect the change of ADK in the setting of I/R injury. Compared with WT group, WT mice with I/R injury had multiple changed candidate genes in ADK related pathways, while

ADK was up-regulated in the setting of I/R (Fig. 1A and B, Fig. S9E). Further analysis to ADK related pathways showed that ADK, DNMT1 and metabolism related genes were significantly changed in the setting of I/R (Fig. 1C). Moreover, correlation analysis showed that ADK had strong negative association with IGF-1, and middle-level negative association with DNA methylation related enzymes (Fig. 1D). Pathways and bioinformatic analysis using datasets from three databases was also performed to identify potential myocardial candidate genes with altered expression in response to I/R. I/R resulted in the altered expression of metabolic genes (Fig. S9A). Further analysis revealed that ADK was significantly increased in the acute period of I/R (less than 24-h) (Supplementary S9C, D), while decreased in the chronic period of I/R (Fig. S9B). Overall, above analysis indicated the association between ADK and other metabolic genes in myocardial I/R.

3.2. Pharmacological ADK inhibition attenuated cardiac I/R injury via increased cardiac adenosine

To assess the role of ADK in myocardial I/R injury, ADK inhibitors were administered to wild-type mice. The mice were intraperitoneally injected with 5-iodotubercidin (5-ITU,1 mg/kg), ABT-702 (1.5 mg/kg), or saline for 7 days before I/R surgery, and the extent of injury in response to I/R was compared in the mice. Evans blue/TTC staining showed that both ADK inhibitors significantly reduced infarction size (Fig. 2A–C). Doppler echocardiography showed that the ADK inhibitors resulted in increased EF and FS values in the mice, indicating that ADK inhibitors treatment preserved cardiac function after I/R surgery (Fig. 2D and E). Metabolomics analysis revealed that ADK inhibition did not affect adenine nucleotide store, concentrations order nor cardiac function (Fig. S10), as reported previously [27].

Because ADK activity and expression have been shown to play a pivotal role in regulating adenosine accumulation [5], we then

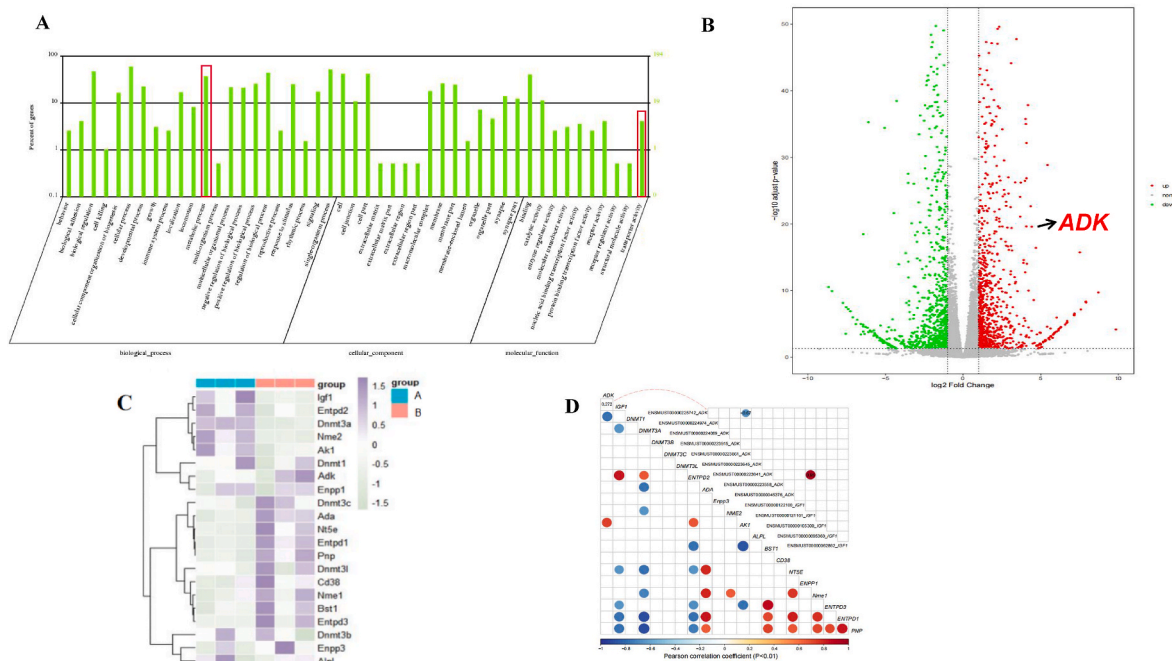


Fig. 1. ADK was identified as a potential candidate gene involved in the metabolic changes during I/R. (A) Pathways with potential difference in the setting of I/R based on RNA-sequencing, the red column marks pathways involved with ADK. (n = 3 per group). (B) Potential candidate genes with changed expression in the setting of I/R based on RNA-sequencing, the bold black arrow marks the position of ADK. (n = 3 per group). Log2 fold change in X axis legend means the expression changes of target genes. Log10 adjust P value means the difference of target genes between groups.(C) Comparison of target genes between WT and WT + I/R group in the setting of 3-h I/R injury, Group A, wild-type mice; Group B, wild-type mice with I/R surgery, other details were demonstrated in the Supplementary Fig. 9. (n = 3 per group). (D) Logistics analysis of ADK to other genes. Red color represents positive association. Blue color represents negative association. Abbreviations in C and D represents the candidate genes with potential difference. (For interpretation of the references to color in this figure legend, the reader is referred to the Web version of this article.)

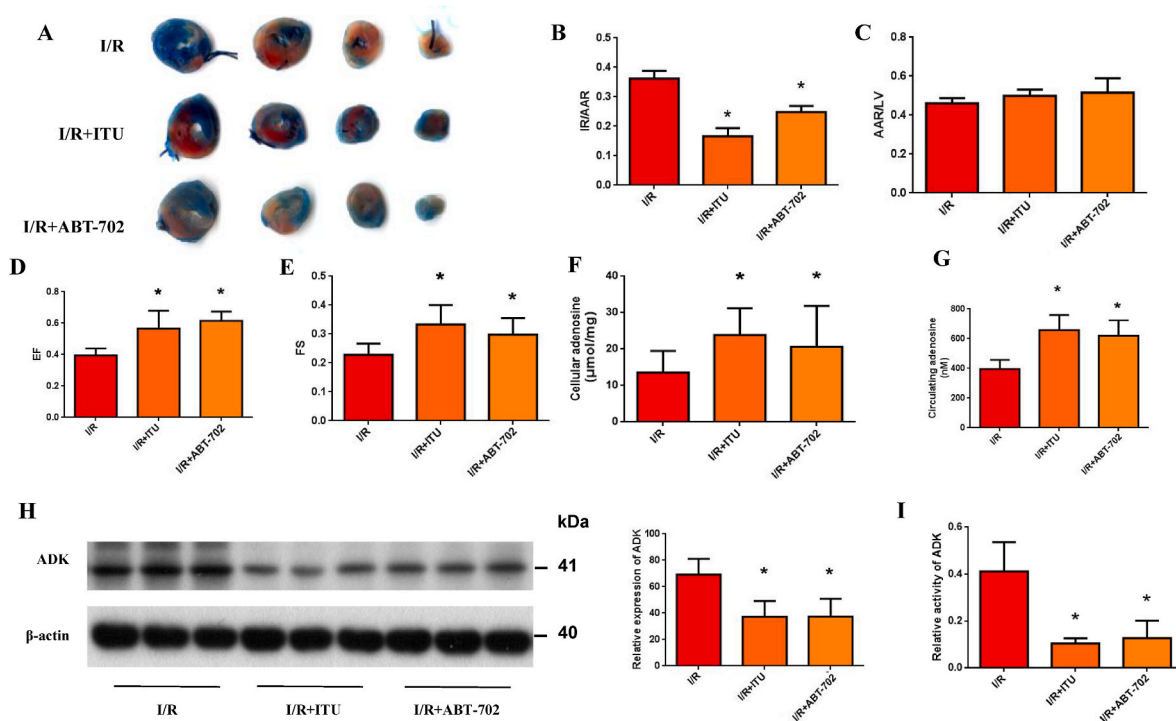


Fig. 2. ADK inhibition attenuated myocardial I/R injury via cardiomyocyte adenosine accumulation in mice. (A) Evans blue/TTC staining of frozen myocardial tissue sections from wild-type mice treated with 5-iodotubercidin (ITU), ABT-702 dihydrochloride (ABT-702), or saline for 7 days prior to I/R surgery. (B) IR/AAR assessed from Evans blue/TTC staining. (n = 5 per group). (C) AAR/LV assessed from Evans blue/TTC staining. (n = 5 per group). (D) Echocardiographic analysis of ejection fraction in mice from the indicated treatment groups (n = 5 per group). (E) Echocardiographic analysis of fractional shortening in mice from the different treatment groups (n = 5 per group). (F) High-performance liquid chromatography of myocardial cellular adenosine levels (n = 5–7 per group). (G) High-performance liquid chromatography of circulating adenosine levels (n = 5–7 per group). (H) Western blot analysis of ADK expression. (I) Analysis of ADK activity. All marks indicated $P < 0.05$, *, † and ‡ to indicate significance versus 1st, 2nd, and 3rd group accordingly. I/R: I/R surgery alone; I/R + ITU: I/R surgery and ITU treatment; I/R + ABT-702: I/R surgery and ABT-702 treatment. (For interpretation of the references to color in this figure legend, the reader is referred to the Web version of this article.)

evaluated the effects of ADK inhibitors on adenosine levels in both isolated cardiomyocytes and peripheral blood. Indeed, ADK inhibition resulted in elevated adenosine levels in cardiomyocytes as well as peripheral blood after I/R surgery (Fig. 2F and G). Interestingly, treatment with ABT-702 and iodotubercidin, which directly inhibit ADK activity, also markedly decreased the ADK protein expression levels and activity after I/R surgery as compared with saline-treated controls (Fig. 2H and I), and 5-ITU maintained ideal specific action on ADK *in vivo* (Fig. S13). The mechanism of ADK inhibitors might be multiple to decrease ADK expression. For 5-Iodotubercidin (5-ITU), an ATP mimetic for ADK, its interference on ATP reaction could further influence the stabilization of ADK protein structure and speed up ADK degradation [28], while ABT-702 had some orders of magnitude selectivity over other sites of adenosine interaction besides ADK. Such effects might be involved in the degradation of ADK [29]. Altogether, these data showed that pharmacological ADK inhibition resulted in increased cardiac adenosine, decreased myocardial injury, and preserved cardiac function after I/R.

3.3. Cardiomyocyte-specific ADK knockout ameliorated myocardial I/R injury via adenosine-induced DNMT1 inhibition

Because ADK inhibition caused adenosine accumulation in the heart, we examined ADK expression in various cells isolated from the hearts of mice after I/R surgery. Specifically, cardiomyocytes, fibroblasts, and endothelial cells were isolated from wild-type mice at 3 and 24 h after I/R surgery. Interestingly, ADK protein content was significantly increased in cardiomyocytes at the 3-h timepoint compared with the sham group; however, the increase was no longer observed at the 24-h timepoint (Fig. 3A), verified by ELISA. No significant differences in ADK levels

were observed in the fibroblasts and endothelial cells at either timepoint after I/R surgery (Fig. 3A). Furthermore, cardiomyocytes exhibited a remarkable decrease in cellular adenosine at the 3-h I/R timepoint, as reported previously, the potential mechanism could be I/R-induced increased HIF transcriptionally repressed ENT1, ENT2 and further decrease cellular adenosine uptake [30,31]. Fibroblasts and endothelial cells, however, did not exhibit significant changes in cellular adenosine levels (Figs. S1A–S1C). These results suggest that increased ADK expression reduces cardiomyocyte adenosine accumulation after I/R.

Based on the above findings, we examined the effect of cardiomyocyte-specific ADK-knockout on tolerance to I/R (details provided in Supplemental Material). After I/R surgery, Evans blue/TTC staining demonstrated reduced infarction sizes (Fig. 3B and E), while echocardiographic analysis revealed preserved cardiac function in cardiomyocyte ADK KO as compared to controls (Fig. 3C and D). TUNEL staining also revealed less apoptotic cells in the myocardial tissues from the ADK-knockout mice compared with those from their wild-type littermates (Fig. 3F). The ADK-knockout mice also exhibited increased cardiomyocyte adenosine accumulation compared with their wild-type littermates, despite similar levels of circulating adenosine. Overall, these findings verified the cardioprotective effects of ADK knockout specifically in cardiomyocytes (Figs. S1D and S1E).

Adenosine accumulation has been shown to inhibit DNMT1 via regulation of the SAM/SAH reaction [32]. Interestingly, we observed that DNMT1 protein expression and activity were strongly diminished in ADK KO hearts after I/R surgery compared with wild-type littermates (Fig. 3G). To examine whether reduced DNMT1 expression played a role in cardioprotection, DNMT1 expression was restored in ADK-knockout hearts via adenoviral transduction. Evans blue/TTC staining

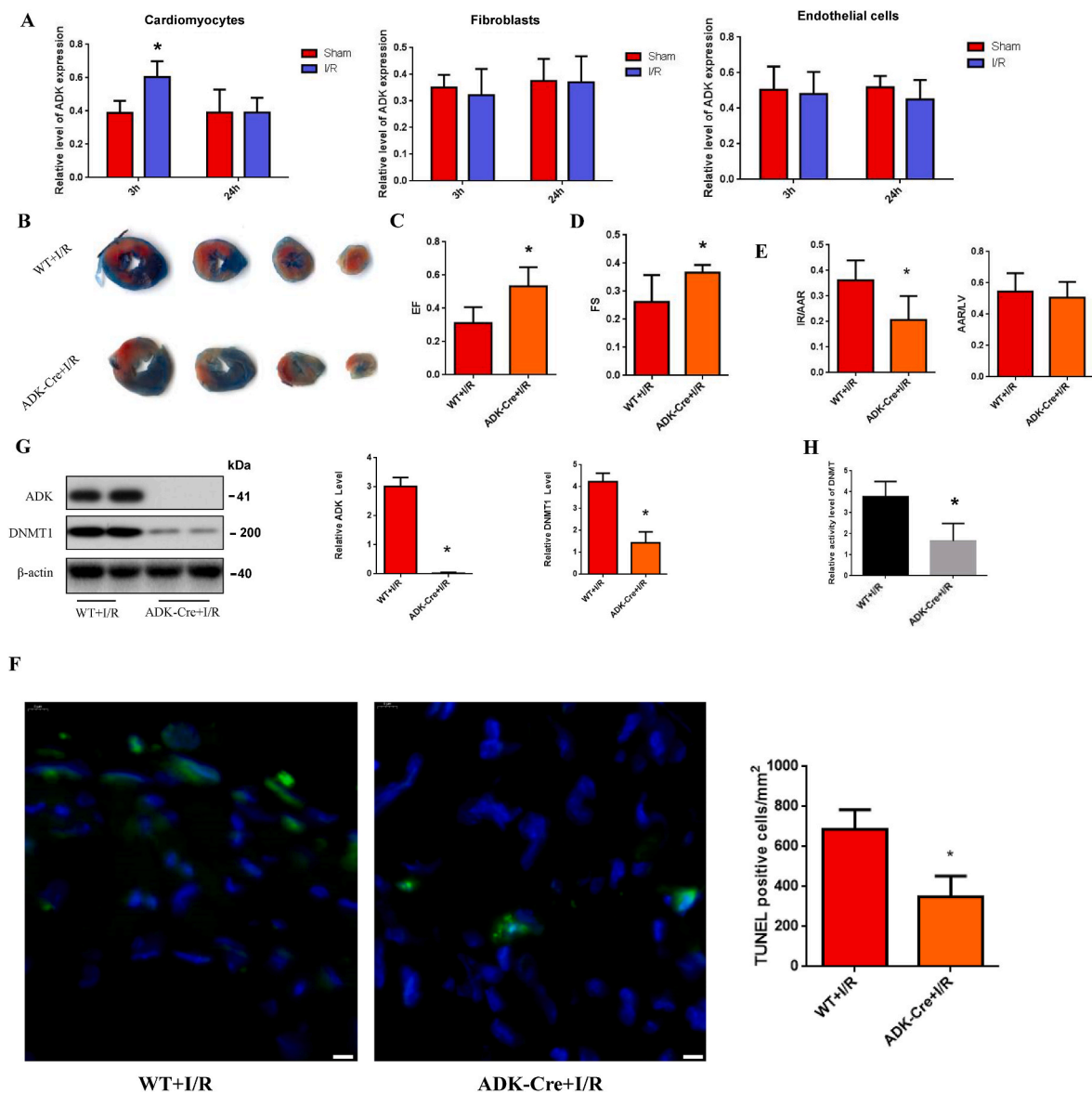


Fig. 3. Cardiomyocyte-specific ADK knockout ameliorated myocardial I/R injury via adenosine-induced DNMT1 inhibition. (A) Detection of ADK expression in different cell types isolated from the hearts of wild-type mice at 3 and 24 h after I/R surgery. (n = 5 per group) (B) Evans blue/TTC staining of myocardial tissue sections from cardiomyocyte-specific ADK-knockout and wild-type mice after I/R surgery. (n = 6 per group). (C) Echocardiographic analysis of ejection fraction in the ADK-knockout and wild-type mice after I/R surgery. (n = 5 per group). (D) Echocardiographic analysis of fractional shortening in the ADK-knockout and wild-type mice after I/R surgery. (n = 5 per group). (E) IR/AAR assessed from the Evans blue/TTC staining. (n = 6 per group). (F) Apoptosis levels assessed by TUNEL staining of the myocardial tissues from the ADK-knockout and wild-type mice after I/R surgery. Bars are 5 μm marked with white color in the merged version. (G) Detection of DNMT1 expression and activity. (n = 5 per group). WT + I/R: wild-type mice with I/R surgery; ADK-Cre + I/R: cardiomyocyte-specific ADK-knockout mice with I/R surgery. All marks indicated P < 0.05, *, † and ‡ to indicate significance versus 1st, 2nd, and 3rd group accordingly. All experiments were repeated 3 times. (For interpretation of the references to color in this figure legend, the reader is referred to the Web version of this article.)

demonstrated that DNMT1 overexpression abrogated the cardioprotective effects of cardiomyocyte-specific ADK knockout in response to I/R (Figs. S1F, H, I and J). In addition, further Western Blot showed that at 3 h post-I/R, there was significant increases of ADK expression in cardiomyocytes compared with sham, while no differences were observed in endotheliums or fibroblast (Fig. S1G). Altogether, these data demonstrated that cardiomyocyte-specific ADK knockout enhanced cardiomyocyte adenosine accumulation and ameliorated myocardial I/R injury by inhibiting the expression of DNMT1.

3.4. Cardiomyocyte-specific ADK knockout increased IGF-1 transcription via regulation of adenosine-associated DNA methylation

Because ADK has been demonstrated to play a role in regulating DNA methylation [5,33] and cardiomyocyte-specific ADK knockout diminished DNMT1 expression, we examined effects of ADK disruption on DNA methylation. MeDIP assay was performed using cardiomyocytes isolated from four groups of mice consisting of either wild-type or ADK-knockout mice with or without I/R surgery (WT, ADK-Cre, WT + I/R, and ADK-Cre + I/R). The results showed that the global DNA methylation of cardiomyocytes in ADK-knockout mice was significantly reduced compared with the wild-type mice, and this hypomethylation was still evident in response to I/R injury (Fig. 4A). Additionally,

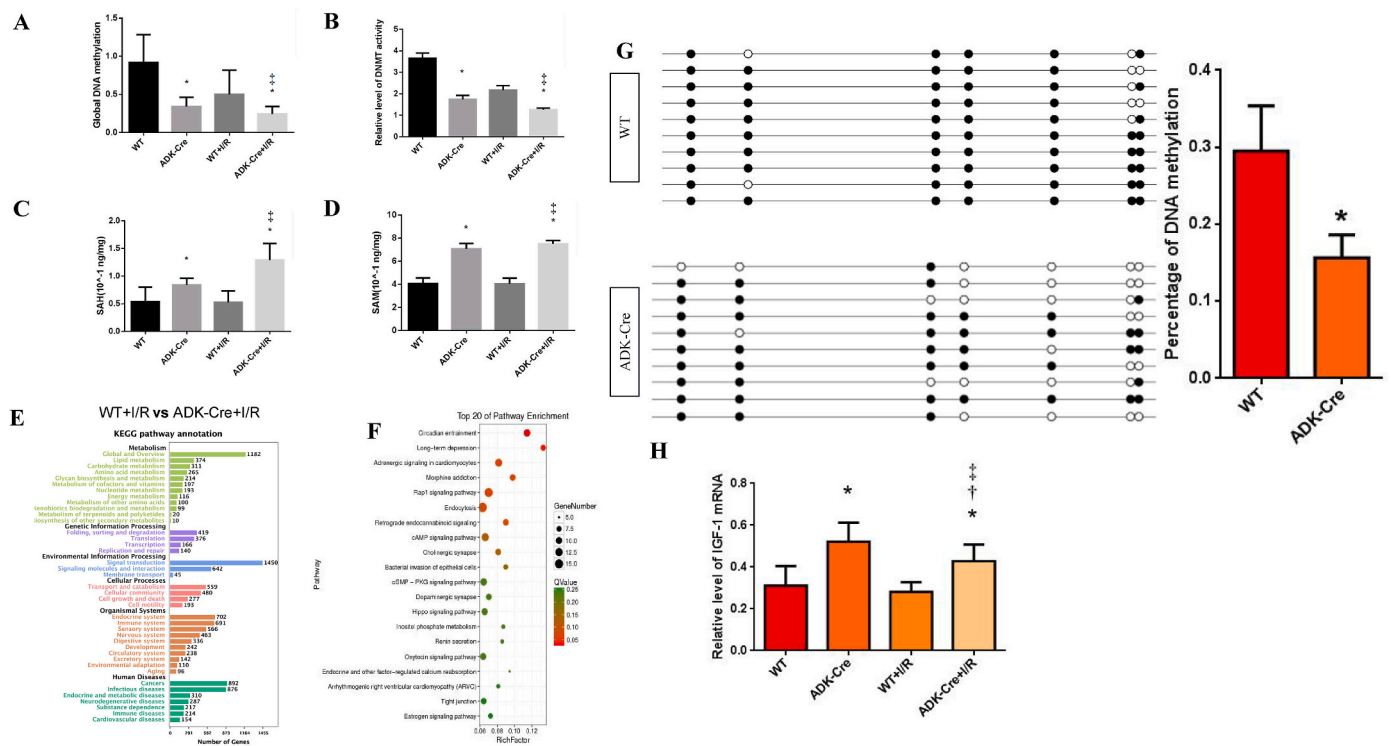


Fig. 4. Cardiomyocyte-specific ADK knockout induced the hypomethylation of genes involved in metabolic pathways and increased IGF-1 transcription via the hypomethylation of its promoter. (A) Global DNA methylation levels assessed by methylated DNA immunoprecipitation (MeDIP) in the hearts of wild-type and cardiac-specific ADK-knockout mice with or without I/R surgery. (n = 6 per group). (B) Relative DNMT1 activity in the hearts of the mice. (n = 5 per group). (C) Quantification of SAH in the hearts of the mice. (n = 5 per group). (D) Quantification of SAM in the hearts of the mice. (n = 5 per group). (E) KEGG analysis of the MeDIP data from the wild-type and ADK-knockout mice after I/R surgery. (n = 5 per group). (F) Pathway enrichment analysis in cardiomyocytes from the ADK-knockout mice after I/R surgery. (n = 5 per group). (G) DNA methylation detected by bisulfite sequencing PCR (BSP) in the IGF-1 promoter. (n = 5 per group). (H) PCR analysis for IGF-1 transcription. (n = 5 per group). For (A)–(D) and (H), WT: wild-type mice with sham surgery; ADK-Cre: cardiomyocyte-specific ADK-knockout mice with sham surgery; WT + I/R: wild-type mice with I/R surgery; ADK-Cre + I/R: cardiomyocyte-specific ADK-knockout mice with I/R surgery. For (E), ADK^{WT} + I/R: wild-type littermates with I/R surgery; ADK^{Myo-KO} + I/R: cardiomyocyte-specific ADK-knockout mice with I/R surgery. For (G), WT: wild-type mice with I/R surgery; ADK-Cre: cardiomyocyte-specific ADK-knockout mice with I/R surgery. All marks indicated P < 0.05, *, † and ‡ to indicate significance versus 1st, 2nd, and 3rd group accordingly. All experiments were repeated 3 times.

cardiomyocyte-specific ADK knockout resulted in decreased DNMT1 activity and elevated levels of SAM and SAH, indicating that it inhibited the transmethylation reaction (Fig. 4B–D). Further analysis of the MeDIP data revealed that cardiomyocyte-specific ADK knockout resulted in the hypomethylation of multiple genes involved in metabolic pathways, including IGF-1 (Fig. 4E and F, Figs. S2A and S2B). These data demonstrated that cardiomyocyte-specific ADK knockout predominantly resulted in the hypomethylation of metabolic genes potentially involved in I/R injury and that IGF-1 was a potential downstream target gene of ADK.

Next, bisulfite sequencing PCR (BSP) was conducted to assess CpG site methylation within the IGF-1 promoter in response to ADK knockout-induced adenosine accumulation (Figs. S2C and S2D). The results revealed that multiple CpG sites were hypomethylated in the cardiomyocyte-specific ADK-knockout mice and that these mice exhibited a significantly lower percentage of DNA methylation in the IGF-1 promoter compared with wild-type mice (Fig. 4G). Furthermore, this DNA hypomethylation resulted in elevated levels of IGF-1 mRNA in the ADK-knockout mice under baseline conditions as well as after I/R surgery (Fig. 4H). Because SAM has been reported to be involved in both DNA and histone methylation and ADK knockout in endothelial cells has been shown to mediate histone methylation [32,34], we assessed the methylation of multiple histone sites. However, no differences were observed for any of the histone sites evaluated in the isolated cardiomyocytes (Fig. S3). This finding indicated that ADK knockout-induced adenosine accumulation did not alter histone methylation via SAM upregulation.

To explore potential effects of adenosine levels, LC-MS was performed in isolated cardiomyocytes. In the setting of I/R injury, compared with wild type mice, ADK knockdown maintained homeostasis of adenosine stores in cardiomyocytes, as verified by decreased AMP, increased ADP and ATP (Figure S8A to D, F). In addition, ADK knockdown did not influence concentration of adenosine in cardiomyocytes (Fig. S8E). Considering that potential impact of adenosine levels on cardiac function via AMPK pathways, further experiments were performed to detect levels of total AMPK and AMPK phosphorylation. Although I/R injury indeed regulated the level of cAMP, the cAMP concentration, total AMPK and AMPK phosphorylation were similar between WT and ADK-Cre mice at baseline or in the setting of I/R (Figs. S8D and G).

Overall, these findings demonstrated that cardiomyocyte-specific ADK knockout decreased DNA methylation, but not histone methylation, in genes involved in metabolic pathways by inhibiting the methyl transfer process and that IGF-1 was a downstream target gene that likely accounted for the cardioprotective effects against I/R injury.

3.5. DNMT1 overexpression abrogated the ADK knockout-induced cardioprotective effects in response to I/R

Adenosine accumulation has been reported to negatively regulate SAHH expression or activity, thus inhibiting the SAH/SAM transmethylation reaction and DNMT1 [4,17,35]. Therefore, we assessed the role of DNMT1 in cardiomyocytes in response to adenosine accumulation during I/R. DNMT1 was overexpressed by lentiviral transduction in

cardiomyocytes isolated from wild-type mice. The cardiomyocytes were cultured under H/R conditions to mimic I/R, and adenosine supplementation was used to induce adenosine accumulation. PCR revealed that adenosine supplementation derepressed myocardial IGF-1 transcription after H/R; however, DNMT1 overexpression abrogated this effect (Fig. 5A). In contrast, IGF-1R expression was not affected by adenosine supplementation or DNMT1 overexpression (Fig. 5B). Further analysis revealed that adenosine supplementation reactivated IGF-1 transcription via the hypomethylation of its promoter, whereas DNMT1 overexpression resulted in the opposite effect (Fig. 5C). However, there were no significant changes in the methylation of the IGF-1R promoter (Fig. 5D). Adenosine supplementation also inhibited the SAH/SAM reaction; However, in the case of overexpressing DNMT1, the reaction from SAM to SAH is enhanced, and in this DNMT1 mediated process, increased consumption of SAM and increased production of SAH were observed. (Fig. 5E–G). In addition, DNMT1 overexpression did not increase adenosine, and it might be that the extra production of adenosine by enhanced SAH might be efficiently metabolized by ADK in wild type cardiomyocytes, which did not induce significant increase of adenosine. Next, Western blot analysis was conducted to analyze the protein expression levels of factors potentially influenced by changes in the SAH/SAM transmethylation reaction, including DNMT1, SAHH, IGF-1, and IGF-1R. Adenosine supplementation resulted in reduced SAHH levels and elevated IGF-1 levels (Fig. 5H). Flow cytometry was used to analyze cellular apoptosis and revealed that adenosine supplementation decreased myocardial cell apoptosis, whereas DNMT1

overexpression increased it (Fig. 5I). In addition, adenosine accumulation significantly decreased the activity of SAHH, while DNMT1 overexpression did not (Fig. 5J).

To further investigate the role of cardiomyocyte-specific ADK knockout during I/R, cardiomyocytes were isolated from the ADK-knockout mice for additional *in vitro* experiments under H/R conditions and with or without DNMT1 overexpression by lentiviral transduction. As expected, cardiomyocyte-specific ADK knockout resulted in remarkable adenosine accumulation and thus elicited similar effects to those observed in response to adenosine supplementation. Furthermore, this effect was abrogated by DNMT1 overexpression (Fig. S4 A to G). In addition, isolation of cardiomyocytes itself did not significantly influence morphology of cardiomyocytes (Fig. S4H). However, 24-h cultivation might influence cellular physiology, but this step is necessary to select qualified adherent cardiomyocytes. Despite the limitation, this method was also used in other laboratory [36]. Altogether, these data demonstrated a negative regulatory effect of DNMT1 on the transcriptional reactivation of IGF-1 resulting from ADK knockout-induced adenosine accumulation.

3.6. Cardiomyocyte adenosine accumulation improved myocardial metabolism after I/R by enhancing the IGF-1 signaling pathway

IGF-1 has been shown to be an important regulatory factor for glucose metabolism via its binding to its receptor [37]. Therefore, we analyzed the protein expression levels of IGF-1 as well as DNMT1 in the

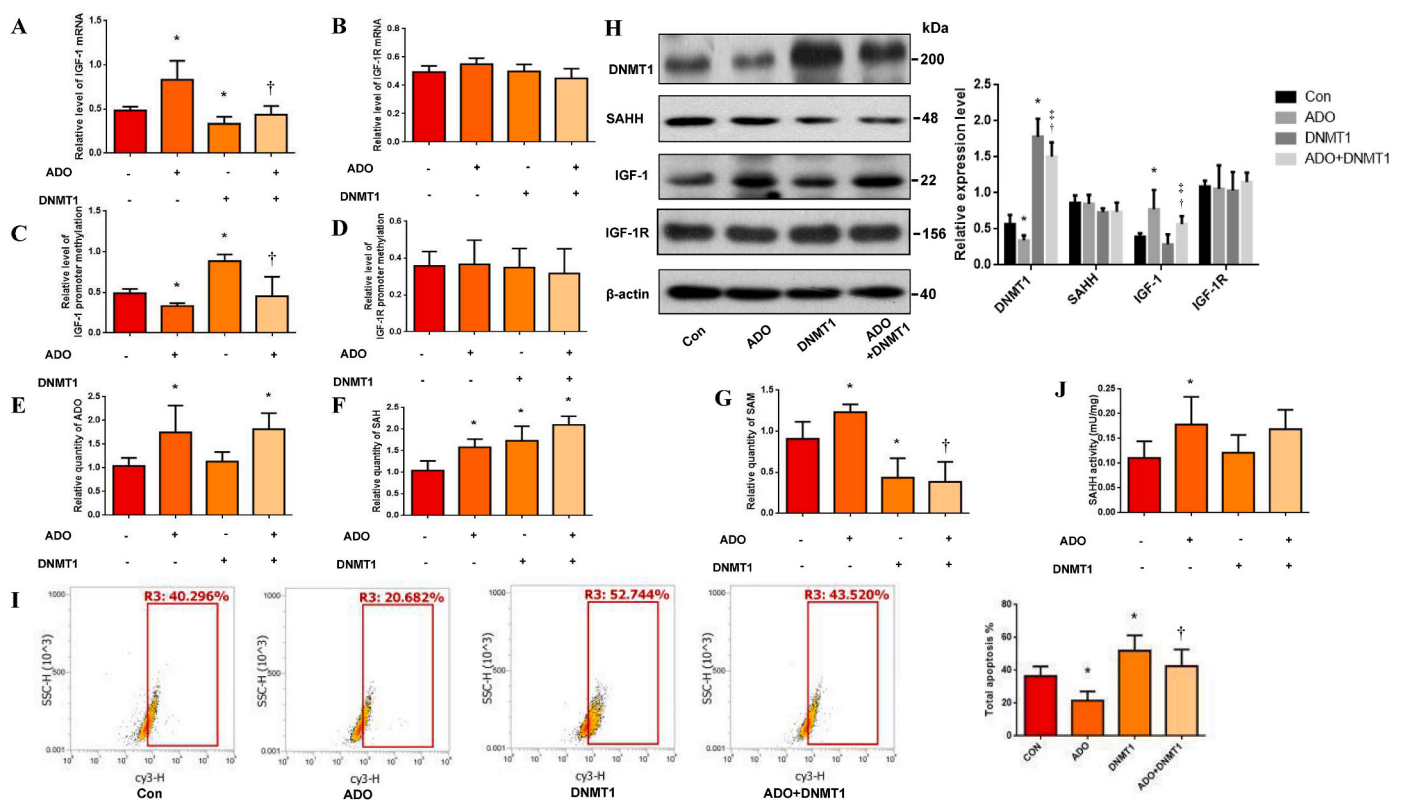


Fig. 5. DNMT1 was a limiting factor for the cardioprotective effects of ADK knockout-induced adenosine accumulation. (A) PCR analysis for IGF-1 transcription. (B) PCR analysis for IGF-1R transcription. (C) DNA methylation detected by bisulfite sequencing PCR (BSP) in the IGF-1 promoter. (D) DNA methylation detected by BSP in the IGF-1R promoter. (E) Quantification of myocardial adenosine levels. (F) SAH levels detected by ELISA. (G) SAM levels detected by ELISA. (H) Western blot analysis of *in vitro* DNMT1, SAHH, IGF-1, and IGF-1R expression (I) *In vitro* apoptosis levels assessed by flow cytometry. (J) SAHH activity in different cells in the presence or absence of ADO, DNMT1. For (A)–(G), ADO: adenosine supplementation, "-" signifies no adenosine supplementation; DNMT1: DNMT1 lentiviral transduction, "-" signifies null vector transduction. For (H) and (I), Con: wild-type cardiomyocytes cultured under hypoxia/reoxygenation (H/R) conditions; DNMT1: wild-type cardiomyocytes cultured under H/R conditions with DNMT1 lentiviral transduction; ADO: wild-type cardiomyocytes cultured under H/R conditions with adenosine supplementation; ADO + DNMT1: wild-type cardiomyocytes cultured under H/R conditions with adenosine supplementation and DNMT1 lentiviral transduction. All marks indicated $P < 0.05$, *, † and ‡ to indicate significance versus 1st, 2nd, and 3rd group accordingly. All experiments were repeated 3 times.

isolated cardiomyocytes. Western blot analysis confirmed elevated levels of IGF-1 and reduced levels of DNMT1 in the cardiomyocytes isolated from the ADK-knockout mice compared with those isolated from wild-type mice (Fig. 6A, Figs. S5A and S5B). PET/CT was performed to explore the metabolic regulatory function of IGF-1 in response to I/R. The results revealed enhanced cardiac glucose uptake in the cardiomyocyte-specific ADK-knockout mice after I/R surgery compared with their wild-type littermates (Fig. 6B). However, no differences were observed in the mice under baseline conditions (Fig. S5C).

To further explore the cardioprotective role of IGF-1 during I/R, additional experiments were performed using an IGF-1 receptor (IGF-1R) inhibitor, OSI-906, to block IGF-1 binding. Evans blue/TTC staining showed that the ADK-knockout mice treated with OSI-906 exhibited larger infarction areas after I/R surgery than the saline-treated controls (Fig. 6C–E). Additionally, IGF-1R inhibition resulted in deteriorated cardiac function (Fig. 6F and G) and reduced cardiac glucose uptake in these mice (Fig. S5D). However, IGF-1R inhibition did not abrogate the cardiomyocyte adenosine accumulation resulting from ADK knockout (Fig. S5E). In addition, ADK knockout decreased fatty acid uptake of heart in the condition of I/R, suggesting that ADK/DNMT1/IGF-1 signaling axis triggered the metabolic switch from fatty acid to glucose metabolism (Fig. S5F). Furthermore, ADK knockout increased mature IGF-1 expression of cardiomyocytes via enhancing IGF-1A transcription (Fig. S5H, Fig. S9F), and OSI-906 treatment mainly inhibit IGF-1R without significant effect on DNMT1 or pINSR (Figs. S5G and I). Altogether these data demonstrated that the ADK/DNMT1/IGF-1 signaling axis was involved in myocardial metabolism and that IGF-1R inhibition abrogated the associated cardioprotective effects of cardiomyocyte-specific ADK knockout. Next, immunofluorescence staining was used to further investigate the spatial relationship of the

myocardial ADK/DNMT1/IGF-1 signaling axis in response to I/R. Associations were observed among the expression of ADK, DNMT1, and IGF-1 (Fig. 6H). Specifically, cardiomyocyte-specific ADK knockout inhibited DNMT1 expression and subsequently enhanced IGF-1 expression in response to I/R. Of note, IGF-1R inhibition did not influence the upstream factors ADK and DNMT1. Therefore, our data demonstrated that cardiomyocyte-specific ADK knockout improved myocardial metabolism after I/R and attenuated I/R injury via enhancement of the ADK/DNMT1/IGF-1 signaling axis.

3.7. IGF-1 is an essential downstream target gene for the metaboloepigenetic effects of cardiomyocyte-specific ADK knockout in response to I/R

Our data demonstrate that ADK/DNMT1 regulates IGF-1 promoter methylation, IGF-1 gene expression and tolerance to I/R, and that IGF-1 signaling is important for the protective effects of ADK KO. To determine whether increased IGF-1 expression is necessary for the cardioprotection observed in ADK KO mice, conditional cardiomyocyte-specific ADK- and IGF-1-double-knockout mice were produced. After I/R surgery, the IGF-1-knockout mice exhibited significantly larger infarction sizes compared with wild-type mice, while ADK/IGF-1-knockout mice exhibited exacerbated I/R injury compared with their ADK-knockout littermates (Fig. 7A–C). Echocardiographic analysis revealed that cardiac function (EF and FS) was improved in the ADK-knockout mice, while deteriorated in IGF-1-knockout mice as compared to WT mice (Fig. 7D and E). Western blot analysis showed that IGF-1 knockout abrogated the inhibitory effect of ADK knockout on DNMT1 and also induced higher levels of apoptotic marker BAX (Fig. 7F) and increased apoptosis *in vivo* (Fig. 7G). Glucose metabolism was evaluated in cardiomyocytes

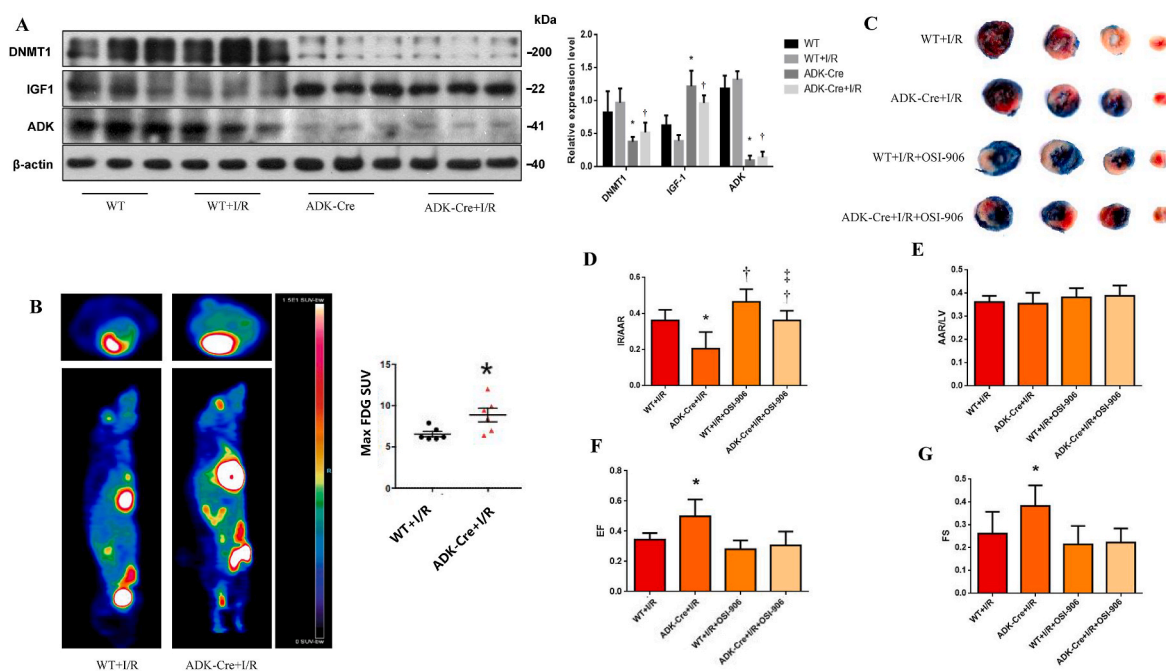


Fig. 6. Cardiomyocyte-specific ADK knockout improved myocardial metabolism via upregulation of the IGF-1-associated pathway after I/R. (A) Western blot analysis of IGF-1, ADK, and DNMT1 expression. (B) PET/CT of cardiac glucose uptake. (n = 5 per group) (C) Evans blue/TTC staining of myocardial tissues from wild-type and ADK-knockout mice after I/R surgery and with or without IGF-1 inhibitor treatment. (D) IR/AAR assessed from the Evans blue/TTC staining (n = 8 per group). (E) AAR/LV assessed from the Evans blue/TTC staining (n = 8 per group). (F) Echocardiographic analysis of ejection fraction in the mice from the different groups (n = 5 per group). (G) Echocardiographic analysis of fractional shortening in the mice from the different groups (n = 5 per group). (H) Immunofluorescence analysis of the spatial distribution. Bars are 50 μm marked with white color in the merged version. (n = 5 per group). All marks indicated P < 0.05, *, † and ‡ to indicate significance versus 1st, 2nd, and 3rd group accordingly. For (A) and (B), WT: wild-type mice with sham surgery; ADK-Cre: cardiomyocyte-specific ADK-knockout mice with sham surgery; WT + I/R: wild-type mice with I/R surgery; ADK-Cre + I/R: cardiomyocyte-specific ADK-knockout mice with I/R surgery. For (C)–(H), WT + I/R: wild-type mice with I/R surgery alone; ADK-Cre + I/R: cardiomyocyte-specific ADK-knockout mice with I/R surgery alone; WT + I/R + OSI-906: wild-type mice with I/R surgery and OSI-906 treatment; ADK-Cre + I/R + OSI-906: cardiomyocyte-specific ADK-knockout mice with I/R surgery and OSI-906 treatment. (For interpretation of the references to color in this figure legend, the reader is referred to the Web version of this article.)

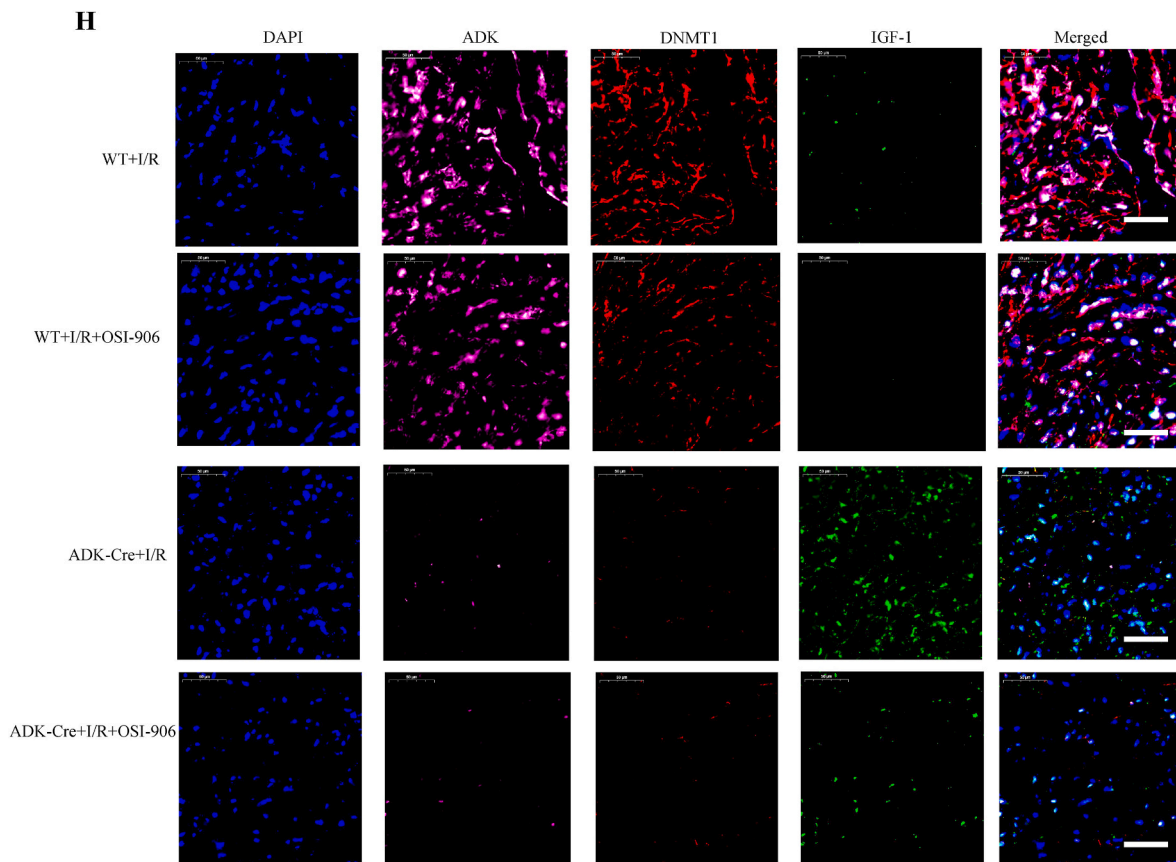


Fig. 6. (continued).

harvested from the mice. The data revealed that both glucose uptake and lactate production were enhanced after cardiomyocyte-specific ADK knockout, and these effects were abrogated by IGF-1 knockout (Fig. 7H and I). Additionally, immunofluorescence assay was used to assess the spatial relationship of the adenosine/DNMT1/IGF-1 axis, and the results were consistent with our hypothesis that endogenous adenosine supplement could regulate expression of key metabolism gene via DNA methylation modification (Fig. 7J). ADK knockout in cardiomyocytes still maintain cardio-protective effect after blocking receptors pharmacologically, suggesting that adenosine accumulation in cardiomyocytes induced by ADK knockdown could protect against I/R injury not only via classic adenosine receptors pathways (Figs. S7A–E). Furthermore, adenosine receptors pharmacological blocking of cardiomyocytes did not affect IGF-1 transcription/translation in either wild type nor ADK-Cre mice (Figs. S7F–H). Altogether, these findings indicated IGF-1 mediates the cardioprotective effects of cardiomyocyte-specific ADK knockout.

3.8. Activation of the ADK/DNMT1/IGF-1 axis improved cellular energy metabolism in cardiomyocytes

Next, we investigated energy metabolism profiles as well as alterations in the associated epigenetic and metabolic factors in isolated cardiomyocytes cultured under H/R conditions. The data showed that both glucose uptake and lactate production were enhanced in the cardiomyocytes isolated from the ADK-knockout mice, and this effect was abrogated by IGF-1 knockout (Fig. 8A and B). In addition, ADK overexpression could enhance the expression of DNMT1 (Fig. S13A). Additionally, elevated adenosine levels in response to ADK knockout were observed as well as alterations in the SAM/SAH reaction, which were consistent with those observed in our animal studies. However, IGF-1 knockout did not affect these alterations in the SAM/SAH reaction,

indicating IGF-1 as a downstream factor in the ADK/DNMT1/IGF-1 axis (Fig. 8C–E, Fig. S13B). Furthermore, assessment of cellular glycolytic function and mitochondrial respiration demonstrated that ADK knockout improved energy metabolism (Figs. S13C and D); however, this effect was abrogated by IGF-1 knockout (Fig. 8F and G, Fig. S6). ADO efflux might vary between cardiomyocyte ADK KO mice and WT mice at baseline or post I/R, Langendorff heart models were performed to measure adenosine efflux in normoxic condition or post 30-min ischemia/60-min, 90-min, 120-min reperfusion by reversed-phase HPLC. There was no difference of adenosine efflux between wild type and cardiomyocyte ADK KO mice at baseline and at various time points of I/R (Figs. S11A–C). Cardiac efflux of adenosine could be influenced by three aspects: cardiac oxygen supply and demand ratio, myocardial oxygen consumption and the formation of extracellular nucleotide. Our study demonstrated that cardiomyocyte of ADK KO mice mainly regulated cellular adenosine level of cardiomyocyte, but did not induce significant direct effect on extracellular or intercellular microenvironment. However, global ADK inhibition by ITU might regulate formation of extracellular nucleotide, which might further increase cardiac efflux of adenosine. Thus, ADO efflux might play an insignificant role in cardiomyocyte ADK KO-mediated effects. The sELISA (abcam, ab244824) results of effluates from Langendorff hearts showed that there is no difference between WT and ADK-Cre mice at baseline or I/R condition (60, 90 and 120 min reperfusion) (Figs. S11D–F). Accordingly, ADK inhibition increased the IGF-1 transcription and enhanced expression of mature IGF-1. The possible reason for why it is not secreted could be explained that most of mature IGF-1 might be used by cardiomyocytes autocrine or paracrine. Altogether, our findings demonstrated epigenetic-metabolic crosstalk in cardiomyocytes cultured under H/R conditions via the ADK/DNMT1/IGF-1 signaling axis. Specifically, cardiomyocyte-specific ADK knockout decreased DNMT1 expression and thereby promoted IGF-1 transcription (Fig. 8H). Overall, these

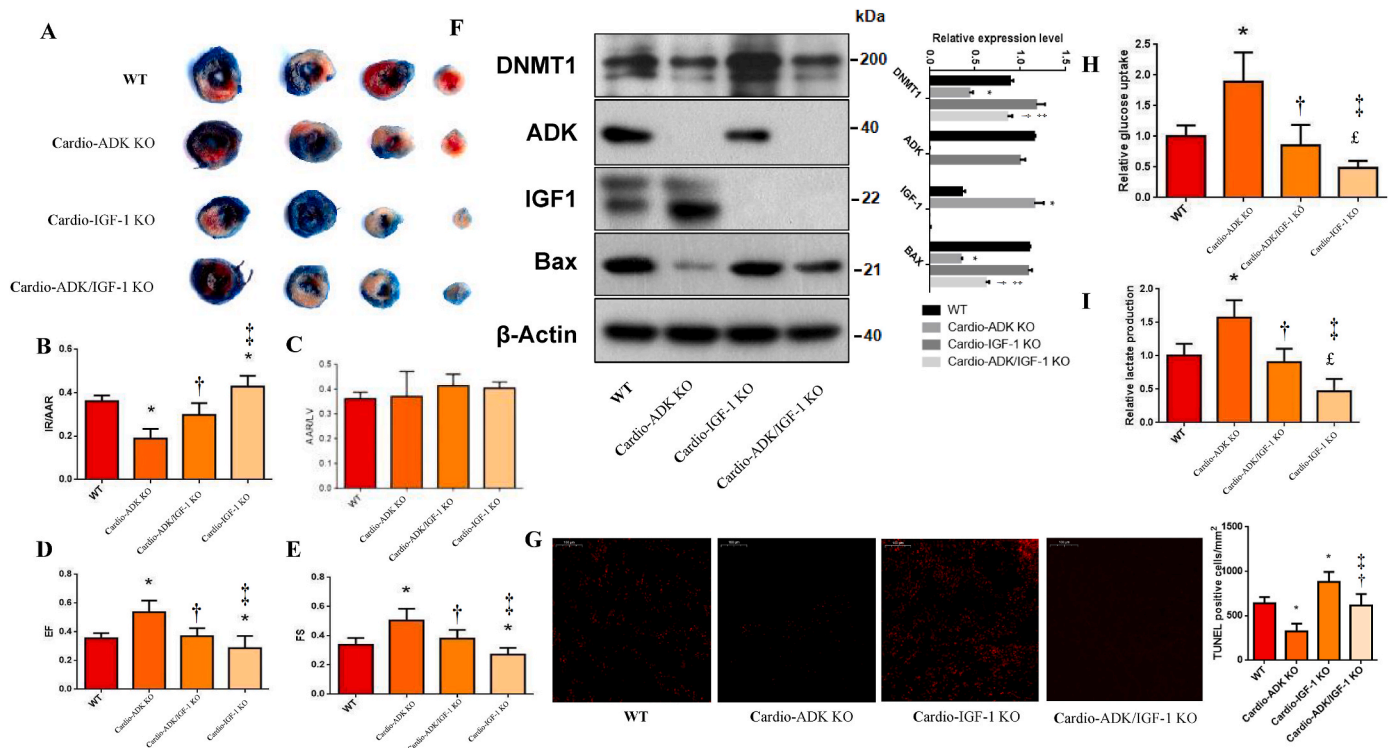


Fig. 7. IGF-1 was identified as a downstream target gene required for the metaboloepigenetic effects of cardiomyocyte-specific ADK knockout in response to I/R (All data in Fig. 7 were under the condition of I/R setting). (A) Evans blue/TTC staining of myocardial tissues from WT, cardio-ADK KO, cardio-IGF-1 KO, cardio-ADK/IGF-1-KO mice (n = 8 per group). (B) IR/AAR assessed from the Evans blue/TTC staining. (C) AAR/LV assessed from the Evans blue/TTC staining. (D) Echocardiographic analysis of ejection fraction in the mice (n = 5 per group). (E) Echocardiographic analysis of fractional shortening in the mice (n = 5 per group). (F) Western blot analysis of IGF-1, BAX, and DNMT1 expression. (G) Detection of *in vivo* ROS levels by DHE staining. (H) Examination of cardiac glucose uptake (n = 5 per group). (I) Examination of cardiac lactate production (n = 5 per group). (J) Immunofluorescence analysis of the spatial distribution of IGF-1, ADK, BAX, and DNMT1 expression. Bars are 50 μm marked with white color in the merged version. All marks indicated P < 0.05, *, † and ‡ to indicate significance versus 1st, 2nd, and 3rd group accordingly. WT: wild-type mice with I/R surgery; cardio-ADK KO: cardiomyocyte-specific ADK-knockout mice with I/R surgery; cardio-ADK/IGF-1-KO: cardiomyocyte-specific ADK/IGF-1-knockout mice with I/R surgery; cardio-IGF-1 KO: cardiomyocyte-specific IGF-1-knockout mice with I/R surgery. All experiments were repeated 3 times. (For interpretation of the references to color in this figure legend, the reader is referred to the Web version of this article.)

findings indicate that myocardial ADK knockout or pharmacological inhibition may improve myocardial energy metabolism and ameliorate I/R injury.

4. Discussion

This is the first study to demonstrate that endogenous adenosine accumulation in cardiomyocytes elicits protective effects against myocardial I/R injury through an epigenetic mechanism. Moreover, our study describes a novel metaboloepigenetic mechanism in which cellular adenosine accumulation increases IGF-1 expression by reducing DNMT1-dependent methylation of the IGF-1 promoter. Importantly, our findings indicate that cardiomyocyte adenosine accumulation significantly improves myocardial energy metabolism via epigenetic reprogramming during I/R. These findings identify cardiomyocyte ADK as novel regulator of epigenetic-metabolic crosstalk during I/R.

Adenosine has been suggested as a feasible therapy to ameliorate I/R injury and remedy “no flow” lesions [9,38]. Previous studies have demonstrated the protective effects of extracellular adenosine and adenosine receptor agonists on ischemia reperfusion, and coronary flow through activation of adenosine receptors [6,39]. Importantly, adenosine has also been shown to reduce infarct size or protect vascular system when administered at reperfusion in humans and animal models [40–42]. While most studies implicate adenosine receptor signaling in the protective effects of adenosine administration, our findings demonstrate for the first time, that cellular adenosine accumulation provides cardioprotection by epigenetic upregulation of cardiomyocyte

IGF-1 expression. The demonstration that restoring DNMT1 expression in ADK KO hearts reversed the protective effects of ADK KO, and that blocking IGF-1 expression or signaling also reversed the protective effects of ADK KO, strongly implicate altered methylation, rather than adenosine receptors, in the cardioprotective effects of ADK KO. Because adenosine is taken up by cardiomyocytes, these findings suggest cellular adenosine accumulation may also contribute to the protective effects of adenosine administration at reperfusion. A recent finding showing that long term administration of adenosine after a myocardial infarction offers significantly greater cardioprotection than a single bolus also supports this suggestion, as it is anticipated that adenosine will be rapidly degraded extracellularly or metabolized once it enters cardiomyocytes [43]. While prolonged coronary infusion of adenosine is not clinically feasible, the finding that reduced DNMT1 expression and its subsequent epigenetic effects are strongly cardioprotective, identify DNMT1 as a novel target for adjunctive therapy of myocardial infarction.

In the heart, ADK metabolizes more than 80% of the total adenosine and thus plays a pivotal role in the regulation of cellular and extracellular adenosine levels [44,45]. Our study identified an important role of ADK inhibition by cardiomyocyte knockdown or pharmacological ADK inhibitors against myocardial I/R injury *in vivo*. Importantly, ADK expression transiently increases after MI, suggesting ADK inhibition at this time may prevent cellular adenosine depletion. Our data strongly indicate that adenosine accumulation in cardiomyocytes is sufficient to elicit cardioprotective effects against I/R injury. In this study, no differences have been observed in the extent of I/R injury between the

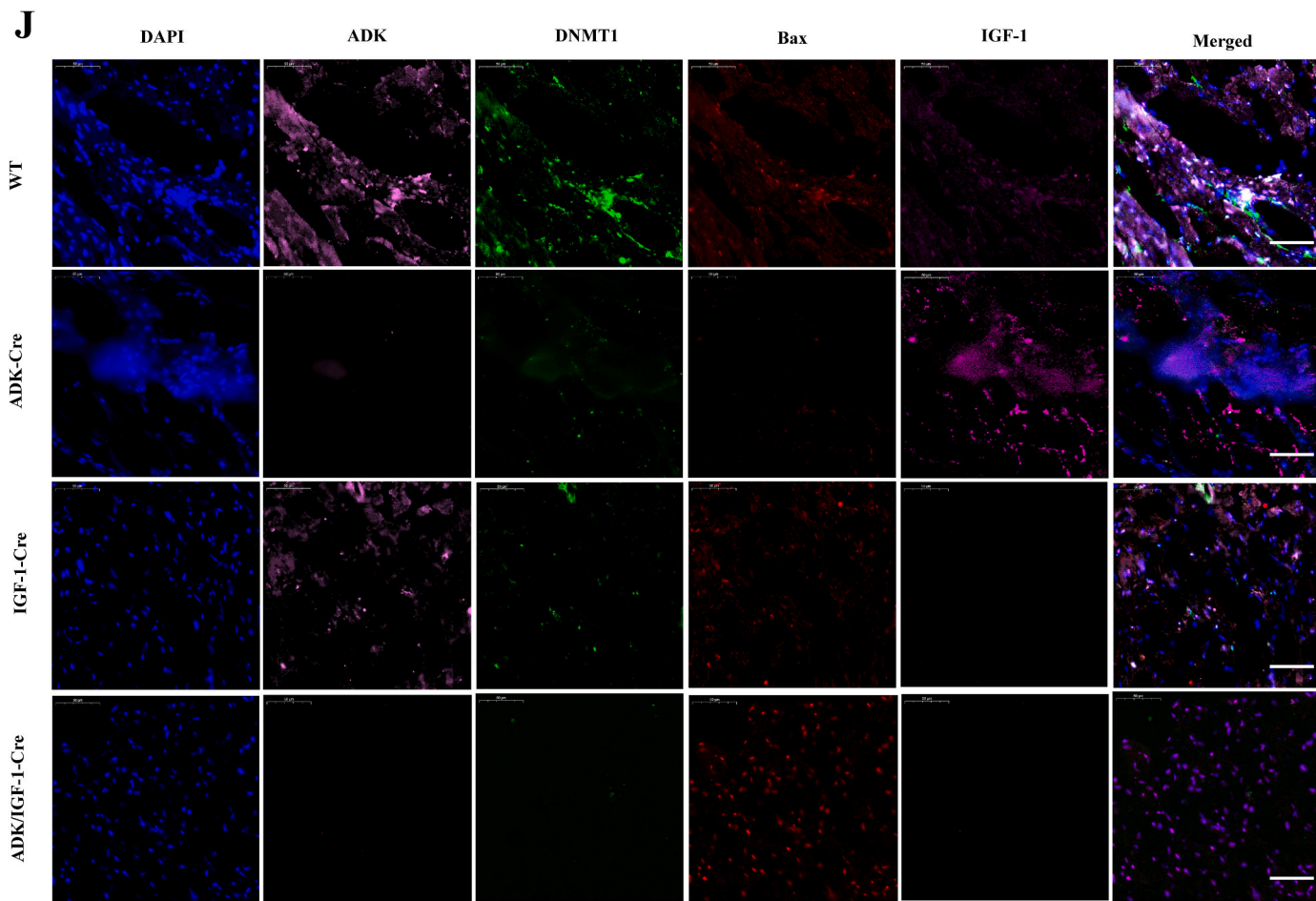


Fig. 7. (continued).

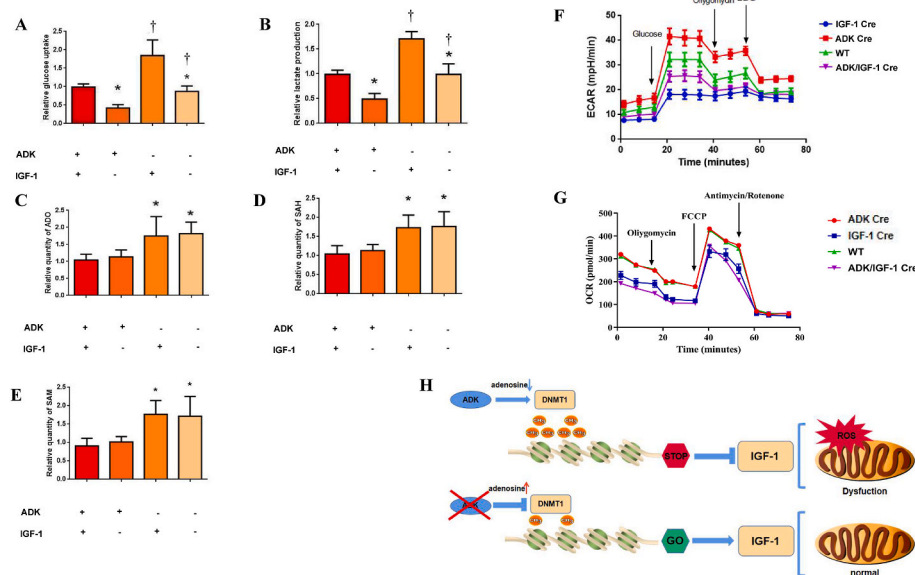


Fig. 8. Activation of the myocardial ADK/DNMT1/IGF-1 signaling axis improved cellular energy metabolism *in vitro*. (A) Examination of myocardial glucose uptake *in vitro*. (n = 5 per group) (B) Examination of myocardial lactate production *in vitro*. (n = 5 per group) (C) Quantification of myocardial adenosine levels. (n = 5 per group) (D) SAH levels detected by ELISA. (n = 5 per group) (E) SAM levels detected by ELISA. (n = 5 per group) (F) Analysis of mitochondrial respiration in cardiomyocytes isolated from mice. (n = 3 per group) (G) Analysis of glycolytic function in cardiomyocytes isolated from mice. (n = 3 per group) (H) Mechanistic model of the myocardial ADK/DNMT1/IGF-1 axis and its downstream metabolic effects. All marks indicated P < 0.05, *, † and ‡ to indicate significance versus 1st, 2nd, and 3rd group accordingly. ADK: wild-type ADK, "-" signifies ADK knockout; IGF-1: wild-type IGF-1, "-" signifies IGF-1 knockout. All experiments were repeated 3 times.

cardiomyocyte-specific ADK-knockout mice and wild-type mice treated with ADK inhibitors, suggesting targeted ADK inhibition as a potential therapeutic strategy to maintain elevated adenosine levels in cardiomyocytes and protect against I/R injury.

Previous studies have demonstrated that ADK inhibition-mediated

adenosine accumulation directly inhibits SAHH activity [46,47]. Adenosine can efficiently bind to SAHH and block the binding between SAHH and NAD⁺, finally resulting in the accumulation of excess SAH [16,18]. Because the accumulation of SAH inhibits methyltransferase activity, cellular adenosine is believed to decrease DNA methylation

through increased SAH levels [33]. However, our findings suggest an additional mechanism by which adenosine accumulation regulates DNA methylation. While SAH can inhibit DNMT1 activity, we found that ADK KO caused a reduction in DNMT1 protein levels. Interestingly, it was recently shown that up-regulation of SAHH activity increased DNMT1 protein expression [48], so it is possible that the epigenetic effects of adenosine-mediated SAHH inhibition stem from both SAH accumulation and diminished DNMT1 expression. However, the finding that histone methylation was not affected by ADK KO, while over-expression of DNMT1 reversed the effects of ADK KO, indicate that loss of DNMT1 plays a greater role than a general reduction in SAM dependent methylation. This is also supported by a previous study showing cardiac protein methylation was not reduced in cardiomyocyte-specific ADK KO [12], and our current study also verified that there were no significant differences of methylation levels in multiple histone modification sites. The mechanism underlying loss of DNMT1 remains to be explored.

Epigenetic modifications, such as DNA methylation, are critical for the regulation of various cellular events, including metabolism, angiogenesis, and apoptosis [49,50]. Our previous studies have demonstrated a direct connection between histone modifications and phospholipid metabolism via metabolites in ischemic cardiomyocytes [22]. Likewise, our latest study has shown that epithelial adenosine accumulation provides a link between DNA methylation and VEGF-induced angiogenesis in endothelial cells and that the associated mechanism involves metabolic cofactors, such as hypoxia, SAM, and acetyl coenzyme A (CoA) [32]. These findings have raised the possibility that adenosine modulates metaboloepigenetic effects to protect against I/R injury in cardiomyocytes. The clinical implication of our study is that targeting ADK inhibition might be a potential strategy to prevent I/R injury. Indeed, current findings have demonstrated that cellular adenosine accumulation, resulting from ADK inhibition, causes the hypomethylation of metabolic genes via DNMT1 inhibition in cardiomyocytes. Previous studies have indicated that IGF-1 improves patient survival by regulating myocardial metabolism in multiple cardiovascular diseases [51, 52]. Moreover, one previous study has proved that induced cardiomyocyte-specific IGF-1 overexpression mitigates I/R injury via phosphatidylinositol kinase related mechanisms, suggesting that IGF-1 is reactivated to improve myocardial energy metabolism in cardiomyocytes [53]. Our study suggested that cardiomyocyte IGF-1 was regulated under ADK-induced metaboloepigenetic effect, and pivotal for mitochondria function. Meanwhile, it might be feasible to target IGF-1 in cardiomyocytes via epigenetic regulation. Therefore, we demonstrate that cardiomyocyte adenosine accumulation increases IGF-1 expression through epigenetic modification of the IGF-1 promoter and identifies the adenosine/DNMT1/IGF-1 axis as a novel metaboloepigenetic target in cardiomyocytes.

In summary, this study demonstrates a novel cardioprotective role for cardiomyocyte adenosine accumulation in attenuating I/R injury through epigenetic modulation of the IGF-1 promoter in cardiomyocytes. Future studies are warranted to explore additional factors related to ADK regulation via epigenetic mechanisms, which could verify additional valuable targets to alleviate mitochondria dysfunction induced by I/R injury. Overall, these findings suggest potential for the clinical application of adenosine-related strategies to target this axis to diminish I/R injury.

Funding

This work was supported by grants from National Natural Science Foundation of China (81900235), National Science Fund for Distinguished Young Scholars (81725002), National Natural Science Foundation of China (Major Program, 82130010), Shanghai Clinical Research Center for Interventional Medicine (19MCI1910300), Basic research projects of Shanghai Science and Technology Commission

(22JC1400500), Innovation Program of Shanghai Municipal Education Commission (2021KJJC-03-1).

Study limitation

Although reported with similar trend by mass spectrometry in other study [27], the concentrations order of cardiomyocytes adenine nucleotides in our study might be influenced by limitation of UPLC-MS/MS, especially for easily degradable or thermally unstable metabolites, certain co-extract components. The detailed adenine nucleotides changes might be further explored with isolated cardiomyocytes. In addition, other genes were possibly regulated under ADK-induced metaboloepigenetic effect except for IGF-1 in cardiomyocytes, which might influence cellular events.

Declaration of competing interest

The authors declare that they have no known competing financial interests or personal relationships that could have appeared to influence the work reported in this paper.

Data availability

Data will be made available on request.

Acknowledgement

Special thanks to GeneMind Biosciences Company Limited, Shenzhen China for providing the RNA-seq sequencing; Thanks to Xin Zhang and Xiaochao Zhao for help with the data analysis and figure preparation.

Appendix A. Supplementary data

Supplementary data to this article can be found online at <https://doi.org/10.1016/j.redox.2023.102884>.

References

- [1] G. Heusch, Myocardial ischaemia-reperfusion injury and cardioprotection in perspective, *Nat. Rev. Cardiol.* 17 (2020) 773–789, <https://doi.org/10.1038/s41569-020-0403-y>.
- [2] A. Ahmadi, G.W. Stone, J. Leipsic, L.J. Shaw, T.C. Villines, M.J. Kern, H. Hecht, D. Erlinge, O. Ben-Yehuda, A. Maehara, E. Arbustini, P. Serruys, H.M. Garcia-Garcia, J. Narula, Prognostic determinants of coronary atherosclerosis in stable ischemic heart disease: anatomy, physiology, or morphology? *Circ. Res.* 119 (2016) 317–329, <https://doi.org/10.1161/CIRCRESAHA.116.308952>.
- [3] J.P. Annes, J.H. Ryu, K. Lam, P.J. Carolan, K. Utz, J. Hollister-Lock, A.C. Arvanites, L.L. Rubin, G. Weir, D.A. Melton, Adenosine kinase inhibition selectively promotes rodent and porcine islet β -cell replication, *Proc. Natl. Acad. Sci. U. S. A.* 109 (2012) 3915–3920, <https://doi.org/10.1073/pnas.1201149109>.
- [4] M.K. Bjursell, H.J. Blom, J.A. Cayuela, M.L. Engvall, N. Lesko, S. Balasubramaniam, G. Brandberg, M. Halldin, M. Falkenberg, C. Jakobs, D. Smith, E. Struys, U. von Döbeln, C.M. Gustafsson, J. Lundeberg, A. Wedell, Adenosine kinase deficiency disrupts the methionine cycle and causes hypermethioninemia, encephalopathy, and abnormal liver function, *Am. J. Hum. Genet.* 89 (2011) 507–515, <https://doi.org/10.1016/j.ajhg.2011.09.004>.
- [5] J. Linden, Role of adenosine in response to vascular inflammation, *Arterioscler. Thromb. Vasc. Biol.* 32 (2012) 843–844, <https://doi.org/10.1161/ATVBAHA.112.247874>.
- [6] M.M. Rabadi, H.T. Lee, Adenosine receptors and renal ischaemia reperfusion injury, *Acta Physiol.* 213 (2015) 222–231, <https://doi.org/10.1111/apha.12402>.
- [7] A.K. Sharma, D.J. LaPar, M.L. Stone, Y. Zhao, C.K. Mehta, I.L. Kron, V.E. Laubach, NOX2 activation of natural killer T cells is blocked by the adenosine A2A receptor to inhibit lung ischemia-reperfusion injury, *Am. J. Respir. Crit. Care Med.* 193 (2016) 988–999, <https://doi.org/10.1164/rccm.201506-1253OC>.
- [8] J. Li, C. Conrad, T.W. Mills, N.K. Berg, B. Kim, W. Ruan, J.W. Lee, X. Zhang, X. Yuan, H.K. Eltzschig, PMN-derived netrin-1 attenuates cardiac ischemia-reperfusion injury via myeloid ADORA2B signaling, *J. Exp. Med.* 218 (2021), <https://doi.org/10.1084/jem.20210008> undefined.

- [9] Ross AM, Gibbons RJ, Stone GW, Kloner RA, Alexander RW, AMISTAD-II Investigators (2005) A randomized, double-blinded, placebo-controlled multicenter trial of adenosine as an adjunct to reperfusion in the treatment of acute myocardial infarction (AMISTAD-II). *J. Am. Coll. Cardiol.* 45:1775-1780. doi: 10.1016/j.jacc.2005.02.061.
- [10] U. Kaya Akca, E. Sag, S. Unal, M. Kasap Duceoglu, Y. Bilginer, S. Ozen, The role of vascular inflammation markers in deficiency of adenosine deaminase 2, *Semin. Arthritis Rheum.* 51 (2021) 839–844, <https://doi.org/10.1016/j.semarthrit.2021.04.013>.
- [11] X. Le, M.V. Negrao, A. Reuben, L. Federico, L. Diao, D. McGrail, M. Nilsson, J. Robichaux, I.G. Munoz, S. Patel, Y. Elamin, Y.H. Fan, W.C. Lee, E. Parra, L. M. Solis Soto, R. Chen, J. Li, T. Karpinet, R. Khairullah, H. Kadara, C. Behrens, B. Sepesi, R. Wang, M. Zhu, L. Wang, A. Vaporciyan, J. Roth, S. Swisher, C. Haymaker, J. Zhang, J. Wang, K.K. Wong, L.A. Byers, C. Bernatchez, J. Zhang, Wistuba II, D.L. Gibbons, E.A. Akbay, J.V. Heymach, Characterization of the immune landscape of EGFR-mutant NSCLC identifies CD73/adenosine pathway as a potential therapeutic target, *J. Thorac. Oncol.* 16 (2021) 583–600, <https://doi.org/10.1016/j.jtho.2020.12.010>.
- [12] J. Fassett, X. Xu, D. Kwak, G. Zhu, E.K. Fassett, P. Zhang, H. Wang, B. Mayer, R. J. Bache, Y. Chen, Adenosine kinase attenuates cardiomyocyte microtubule stabilization and protects against pressure overload-induced hypertrophy and LV dysfunction, *J. Mol. Cell. Cardiol.* 130 (2019) 49–58, <https://doi.org/10.1016/j.yjmcc.2019.03.015>.
- [13] A. Bahreyni, M. Khazaei, M. Rajabian, M. Ryzhikov, A. Avan, S. Hassanian, Therapeutic potency of pharmacological adenosine receptor agonist/antagonist in angiogenesis, current status and perspectives, *J. Pharm. Pharmacol.* 70 (2) (2018) 191–196, <https://doi.org/10.1111/jphp.12844>.
- [14] Y. Zhang, B. Wernly, X. Cao, J. Mustafa, Y. Tang, Z. Zhou, Adenosine and adenosine receptor-mediated action in coronary microcirculation, *Basic Res. Cardiol.* 116 (1) (2021) 22, <https://doi.org/10.1007/s00395-021-00859-7>.
- [15] Michael A. Zimmerman, E. Tak, F. Ehrentauf Stefan, M. Kaplan, A. Giebler, T. Weng, D. Choi, R. Blackburn Michael, I. Kam, K. Eltzschig Holger, A. Grenz, Equilibrative nucleoside transporter (ENT)-1-dependent elevation of extracellular adenosine protects the liver during ischemia and reperfusion, *Hepatology* 58 (5) (2013) 1766–1778, <https://doi.org/10.1002/hep.26505>.
- [16] K. Kroll, U.K. Decking, K. Dreikorn, J. Schradler, Rapid turnover of the AMP-adenosine metabolic cycle in the Guinea pig heart, *Circ. Res.* 73 (1993) 846–856, <https://doi.org/10.1161/01.res.73.5.846>.
- [17] I. Baric, K. Fumic, B. Glenn, M. Cuk, A. Schulze, J.D. Finkelstein, S.J. James, V. Mejaski-Bosnjak, L. Pazanin, I.P. Pogribny, M. Rados, V. Sarnavka, M. Scukanec-Spoljar, R.H. Allen, S. Stabler, L. Uzelac, O. Vugrek, C. Wagner, S. Zeisel, S. H. Mudd, S-adenosylhomocysteine hydrolase deficiency in a human: a genetic disorder of methionine metabolism, *Proc. Natl. Acad. Sci. U. S. A.* 101 (2004) 4234–4239, <https://doi.org/10.1073/pnas.0400658101>.
- [18] M. Barroso, D. Kao, H.J. Blom, I. Tavares de Almeida, R. Castro, J. Loscalzo, D. E. Handy, S-adenosylhomocysteine induces inflammation through NFκB: a possible role for EZH2 in endothelial cell activation, *Biochim. Biophys. Acta* 1862 (2016) 82–92, <https://doi.org/10.1016/j.bbdis.2015.10.019>.
- [19] E.S. Oh, A. Petronis, Origins of human disease: the chrono-epigenetic perspective, *Nat. Rev. Genet.* 22 (2021) 533–546, <https://doi.org/10.1038/s41576-021-00348-6>.
- [20] F. Vaura, J. Palmu, J. Aittokallio, A. Kauko, T. Niiranen, Genetic, molecular, and cellular determinants of sex-specific cardiovascular traits, *Circ. Res.* 130 (4) (2022) 611–631, <https://doi.org/10.1161/CIRCRESAHA.121.319891>.
- [21] W. Tian, H. Xu, F. Fang, Q. Chen, Y. Xu, A. Shen, Brahma-related gene 1 bridges epigenetic regulation of proinflammatory cytokine production to steatohepatitis in mice, *Hepatology* 58 (2013) 576–588, <https://doi.org/10.1002/hep.26207>.
- [22] P. Wang, F. Fan, X. Li, X. Sun, L. Ma, J. Wu, C. Shen, H. Zhu, Z. Dong, C. Wang, S. Zhang, X. Zhao, X. Ma, Y. Zou, K. Hu, A. Sun, J. Ge, Riboflavin attenuates myocardial injury via LSD1-mediated cross-talk between phospholipid metabolism and histone methylation in mice with experimental myocardial infarction, *J. Mol. Cell. Cardiol.* 115 (2018) 115–129, <https://doi.org/10.1016/j.yjmcc.2018.01.006>.
- [23] M.B. Glier, T.J. Green, A.M. Devlin, Methyl nutrients, DNA methylation, and cardiovascular disease, *Mol. Nutr. Food Res.* 58 (2014) 172–182, <https://doi.org/10.1002/mnfr.201200636>.
- [24] S. Imai, C.M. Armstrong, M. Kaeberlein, L. Guarente, Transcriptional silencing and longevity protein Sir2 is an NAD-dependent histone deacetylase, *Nature* 403 (2000) 795–800, <https://doi.org/10.1038/35001622>.
- [25] H. Shi, Y. Gao, Z. Dong, J. Yang, R. Gao, X. Li, S. Zhang, L. Ma, X. Sun, Z. Wang, F. Zhang, K. Hu, A. Sun, J. Ge, GSDMD-mediated cardiomyocyte pyroptosis promotes myocardial I/R injury, *Circ. Res.* 129 (2021) 383–396, <https://doi.org/10.1161/CIRCRESAHA.120.318629>.
- [26] H. Jiang, D. Jia, B. Zhang, W. Yang, Z. Dong, X. Sun, X. Cui, L. Ma, J. Wu, K. Hu, A. Sun, J. Ge, Exercise improves cardiac function and glucose metabolism in mice with experimental myocardial infarction through inhibiting HDAC4 and upregulating GLUT1 expression, *Basic Res. Cardiol.* 115 (2020) 28, <https://doi.org/10.1007/s00395-020-0787-1>.
- [27] D. Shimura, G. Nakai, Q. Jiao, K. Osanai, K. Kashikura, K. Endo, T. Soga, N. Goda, S. Minamisawa, Metabolomic profiling analysis reveals chamber-dependent metabolite patterns in the mouse heart, *Am. J. Physiol. Heart Circ. Physiol.* 305 (4) (2013) H494–H505, <https://doi.org/10.1152/ajpheart.00867.2012>.
- [28] S. Sandau, M. Yahya, R. Bigej, L. Friedman, B. Saleumvong, D. Boison, Transient use of a systemic adenosine kinase inhibitor attenuates epilepsy development in mice, *Epilepsia* 60 (4) (2019) 615–625, <https://doi.org/10.1111/epi.14674>.
- [29] G. Wölkart, H. Stessel, E. Fassett, E. Teschl, K. Friedl, M. Trummer, A. Schrammel, A. Kollau, B. Mayer, J. Fassett, Adenosine kinase (ADK) inhibition with ABT-702 induces ADK protein degradation and a distinct form of sustained cardioprotection, *Eur. J. Pharmacol.* 927 (2022), 175050, <https://doi.org/10.1016/j.ejphar.2022.175050>.
- [30] S. Morote-Garcia, D. Köhler, M. Roth, V. Mirakaj, T. Eldh, K. Eltzschig, P. Rosenberger, Repression of the equilibrative nucleoside transporters dampens inflammatory lung injury, *Am. J. Respir. Cell Mol. Biol.* 49 (2) (2013) 296–305, <https://doi.org/10.1165/rcmb.2012-0457OC>.
- [31] B. Rose, Z. Naydenova, A. Bang, A. Ramadan, J. Klawitter, K. Schram, G. Sweeney, A. Grenz, H. Eltzschig, J. Hammond, D. Choi, R. Coe, Absence of equilibrative nucleoside transporter 1 in ENT1 knockout mice leads to altered nucleoside levels following hypoxic challenge, *Life Sci.* 89 (null) (2011) 621–630, <https://doi.org/10.1016/j.lfs.2011.08.007>.
- [32] Y. Xu, Y. Wang, S. Yan, Y. Zhou, Q. Yang, Y. Pan, X. Zeng, X. An, Z. Liu, L. Wang, J. Xu, Y. Cao, D.J. Fulton, N.L. Weintraub, Z. Bagi, M.N. Hoda, X. Wang, Q. Li, M. Hong, X. Jiang, D. Boison, C. Weber, C. Wu, Y. Huo, Cellular adenosine regulates epigenetic programming in endothelial cells to promote angiogenesis, *EMBO Mol. Med.* 9 (2017) 1263–1278, <https://doi.org/10.1525/emmm.201607066>.
- [33] S. Lee, A.C. Doxey, B.J. McConkey, B.A. Moffatt, Nuclear targeting of methyl-recycling enzymes in *Arabidopsis thaliana* is mediated by specific protein interactions, *Mol. Plant* 5 (2012) 231–248, <https://doi.org/10.1093/mp/ssr083>.
- [34] Y. Xu, Y. Wang, S. Yan, Q. Yang, Y. Zhou, X. Zeng, Z. Liu, X. An, H.A. Toque, Z. Dong, X. Jiang, D.J. Fulton, N.L. Weintraub, Q. Li, Z. Bagi, M. Hong, D. Boison, C. Wu, Y. Huo, Regulation of endothelial cellular adenosine via adenosine kinase epigenetically modulates vascular inflammation, *Nat. Commun.* 8 (2017) 943, <https://doi.org/10.1038/s41467-017-00986-7>.
- [35] J. Linden, F. Koch-Nolte, G. Dahl, Purine release, metabolism, and signaling in the inflammatory response, *Annu. Rev. Immunol.* 37 (2019) 325–347, <https://doi.org/10.1146/annurev-immunol-051116-052406>.
- [36] M. Ackers-Johnson, Y.Q. Li, P. Holmes, S. O'Brien, Da Pavlovic, S. Foo, A simplified, langedorff-free method for concomitant isolation of viable cardiac myocytes and nonmyocytes from the adult mouse heart, *Circ. Res.* 119 (8) (2016) 909–920, <https://doi.org/10.1161/CIRCRESAHA.116.309202>.
- [37] R. Troncoso, C. Ibarra, J.M. Vicencio, E. Jaimovich, S. Lavandro, New insights into IGF-1 signaling in the heart, *Trends Endocrinol. Metabol.* 25 (2014) 128–137, <https://doi.org/10.1016/j.tem.2013.12.002>.
- [38] R.A. Kloner, M.B. Forman, R.J. Gibbons, A.M. Ross, R.W. Alexander, G.W. Stone, Impact of time to therapy and reperfusion modality on the efficacy of adenosine in acute myocardial infarction: the AMISTAD 2 trial, *Eur. Heart J.* 27 (2006) 2400–2405, <https://doi.org/10.1093/eurheartj/ehl094>.
- [39] J.H. Mehaffey, D. Money, E.J. Charles, S. Schubert, A.F. Piñeros, D. Wu, S. V. Bontha, R. Hawkins, N.R. Teman, V.E. Laubach, V.R. Mas, C.G. Tribble, D. G. Maluf, A.K. Sharma, Z. Yang, I.L. Kron, M.E. Roesser, Adenosine 2A receptor activation attenuates ischemia reperfusion injury during extracorporeal cardiopulmonary resuscitation, *Ann. Surg.* 269 (2019) 1176–1183, <https://doi.org/10.1097/SLA.0000000000002685>.
- [40] Mangano DT, Miao Y, Tudor IC, Dietzel C, Investigators of the multicenter study of perioperative ischemia (McSPI) research group, ischemia research and education foundation (IREF) (2006) post-reperfusion myocardial infarction: long-term survival improvement using adenosine regculation with acadesine. *J. Am. Coll. Cardiol.* 48:206-214. doi:10.1016/j.jacc.2006.04.044.
- [41] R. Salie, A. Moolman, A. Lochner, The mechanism of beta-adrenergic preconditioning: roles for adenosine and ROS during triggering and mediation, *Basic Res. Cardiol.* 107 (5) (2012) 281, <https://doi.org/10.1007/s00395-012-0281-5>.
- [42] M. Zhang, X. Zeng, Q. Yang, J. Xu, Z. Liu, Y. Zhou, Y. Cao, X. Zhang, X. An, Y. Xu, L. Huang, Z. Han, T. Wang, C. Wu, D.J. Fulton, N.L. Weintraub, M. Hong, Y. Huo, Ablation of myeloid ADK (adenosine kinase) epigenetically suppresses atherosclerosis in ApoE (apolipoprotein E deficient) mice, *Arterioscler. Thromb. Vasc. Biol.* 38 (2018) 2780–2792, <https://doi.org/10.1161/ATVBAHA.118.311806>.
- [43] T. Yetgin, A. Uitterdijk, M. Te Lintel Hekker, D. Merkus, I. Krabbendam-Peters, H. M.M. van Beusekom, R. Falotico, P.W. Serruys, O.C. Manintveld, R.M. van Geuns, F. Zijlstra, D.J. Duncker, Limitation of infarct size and No-reflow by intracoronary adenosine depends critically on dose and duration, *JACC Cardiovasc. Interv.* 8 (2015) 1990–1999, <https://doi.org/10.1016/j.jcin.2015.08.033>.
- [44] A. Deussen, M. Stappert, S. Schafer, M. Kelm, Quantification of extracellular and cellular adenosine production: understanding the transmembranous concentration gradient, *Circulation* 99 (1999) 2041–2047, <https://doi.org/10.1161/01.cir.99.15.2041>.
- [45] M.R. Mehaffey, M.B. Cammarata, J.S. Brodbelt, Tracking the catalytic cycle of adenylate kinase by ultraviolet photodissociation mass spectrometry, *Anal. Chem.* 90 (2018) 839–846, <https://doi.org/10.1021/acs.analchem.7b03591>.
- [46] D. Boison, Adenosine kinase: exploitation for therapeutic gain, *Pharmacol. Rev.* 65 (2013) 906–943, <https://doi.org/10.1124/pr.112.006361>.
- [47] D. Kloor, H. Osswald, S-Adenosylhomocysteine hydrolase as a target for cellular adenosine action, *Trends Pharmacol. Sci.* 25 (2004) 294–297, <https://doi.org/10.1016/j.tips.2004.04.004>.
- [48] P. Wu, Y. Tang, X. Fang, C. Xie, J. Zeng, W. Wang, S. Zhao, Metformin suppresses hypopharyngeal cancer growth by epigenetically silencing long non-coding RNA SNHG7 in FaDu cells, *Front. Pharmacol.* 10 (undefined) (2019) 143, <https://doi.org/10.3389/fphar.2019.00143>.
- [49] B.A. Garcia, Z. Luka, L.V. Loukachevitch, N.V. Bhanu, C. Wagner, Folate deficiency affects histone methylation, *Med. Hypotheses* 88 (2016) 63–67, <https://doi.org/10.1016/j.mehy.2015.12.027>.

- [50] D. Hamdane, H. Grosjean, M. Fontecave, Flavin-dependent methylation of RNAs: complex chemistry for a simple modification, *J. Mol. Biol.* 428 (2016) 4867–4881, <https://doi.org/10.1016/j.jmb.2016.10.031>.
- [51] O. Saetrum, P.H. Wang, IGF-I is a matter of heart, *Growth Hormone IGF Res.* 15 (2005) 89–94, <https://doi.org/10.1016/j.ghir.2005.02.002>.
- [52] D. von Lewinski, K. Voss, S. Hülsmann, H. Kögler, B. Pieske, Insulin-like growth factor-1 exerts Ca²⁺-dependent positive inotropic effects in failing human myocardium, *Circ. Res.* 92 (2003) 169–176, <https://doi.org/10.1161/01.res.0000051885.70159.12>.
- [53] H. Otani, T. Yamamura, Y. Nakao, R. Hattori, H. Kawaguchi, M. Osako, H. Imamura, Insulin-like growth factor-I improves recovery of cardiac performance during reperfusion in isolated rat heart by a wortmannin-sensitive mechanism, *J. Cardiovasc. Pharmacol.* 35 (2) (2000) 275–281, <https://doi.org/10.1097/00005344-200002000-00015>.